Table 2 Virological response to interferon treatment in HIV–HCV co-infected patients

Genotype	Viral load (High : Low)†	Response			Total
		SVR	ETR	NR	
(a) Response to interferon treatment in total (with or without ribavirin)					
1	9:6	7 (33.3%)	1	13	21
2	5:3	4 (40.0%)	2	4	10
3	5:1	5 (62.5%)	1	2	8
4	1:0	0	1	0	1
Mixed	5:1	2 (33.3%)	3	1	6
Others	6:2	8 (57.1%)	3	3	14
Total	31:13	26 (43.4%)	11	23	60
(b) Response to ribavirin/interferon combination therapy including peginterferon					
1	8:2	2 (15.3%)	0	11	13
2	1:2	1 (25.0%)	0	3	4
3	4:1	4 (66.7%)	1	1	6
4	1:0	0	1	0	1
Mixed	4:1	1 (20.0%)	3	1	5
Others	3:0	3 (50.0%)	1	2	6
Total	21:6	11 (31.4%)	6	18	35

†Viral loads are available in only a subset of patients. High viral load: more than 1 Meq/mL by Branched DNA-probe assay or more than 100 KIU/mL by Amplicor monitor assay.
ETR, end of treatment virological response; NR, no virological response; SVR, sustained virological response.

counts in the patients who achieved SVR was significantly larger than that in the non-IFN-treated patients ($P < 0.05$, Table 4).

No symptoms of hepatic failure (ascites or hepatic encephalopathy) were observed in the 60 IFN-treated patients while they were observed in six of the 98 non-IFN-treated patients. HCC was found in one IFN-treated patient after SVR, while it was found in two non-IFN-treated patients (Table 4).

Impact of HAART on liver function and associated complications (Table 5)

Information on HAART was available in 292 patients. The mean observation periods were 8.4 ± 4.2 years in 234 patients on HAART, and 9.8 ± 6.0 years in 58 patients not on HAART. Changes in the levels of albumin, bilirubin or platelet were similar between the two groups (statistically not significant). The morbidities of hepatic decompensation symptoms (ascites and hepatic encephalopathy) and HCC were not significantly different between the two groups. In total, nine patients had hepatic decompensation and seven had HCC, and the average age of such patients was 41.1 ± 14.0 years, which was much younger than that of HCV mono-infected patients with the same complications.[9]

DISCUSSION

IN THE CURRENT study, the features of liver disease in HIV–HCV co-infected patients in Japan were analyzed. The determination of HCV genotypes revealed that genotype 3 or 4, which is rarely seen in HCV mono-infected patients in Japan,[10] was found in a substantial fraction of HIV-infected patients. In addition, some of these patients were infected with HCV of mixed genotypes. These results are compatible with the fact that HCV is transmitted through imported blood products that were contaminated by HCV, as is the case with HIV infection.[11] Infection by HCV of mixed genotypes may reflect frequent administrations of blood products of different lots.

We evaluated the response rate to IFN treatment in HIV–HCV co-infected patients in Japan. Because the IFN treatment protocol varied between facilities, it was not easy to evaluate the effects of the treatments including IFN in this cohort. However, the regimen of ribavirin/IFN combination therapy was similar between the hospitals: the treatment period was 24 weeks in patients with HCV genotypes 2 and 3, and 48 weeks in those with HCV of other genotypes when either pegylated or standard IFN in combination with ribavirin was used.[12] Therefore, it may be possible to estimate the effect

Table 3 Clinical backgrounds of patients who spontaneously cleared HCV in HIV-infected patients

Patient no.	Age	Sex	Transmission route	Observation period (years)	HCV-RNA (KIU/mL)	HCV genotype	HIV-RNA ($\times 10^2$/mL)	WBC (/μL)	CD4+ T cells (/μL)	Platelets ($\times 10^4$/mL)	ALT (U/l)	HAART
1	33	M	Transfusion	8.8	290	ND	200 000	4500	5	26.3	21	Yes
2	31	M	MSM	2.3	Positive†	ND	13 000	5760	931	22.7	29	Yes
3	27	M	Transfusion	9.3	>850	3a	180 000	4000	51	10.1	84	Yes
4	53	M	Transfusion	4.5	Positive†	1a	20 000	4800	296	35.4	24	No
5	22	M	Transfusion	7.8	220	ND	990	5500	125	33.1	44	Yes

†Positive: HCV-RNA was positive by qualitative PCR, but was not quantitatively determined.
ALT, aminotransferase; HAART, highly active anti-retroviral therapy; HCV, hepatitis C virus; HIV, human immunodeficiency virus; MSM, men who have sex with men; ND, not determined; WBC, white blood cells.

Table 4 Changes in clinical parameters and IFN treatment in HIV–HCV co-infected patients

	Outcome of IFN treatment	Number	Observation period (years)	⊿Albumin†	⊿Bilirubin‡	⊿Platelet§	Ascites/ encephalopathy	HCC
IFN-treated patients		60	9.5 ± 5.0	0.05 ± 0.42	0.08 ± 0.38*	0.06 ± 1.13	0	1
	SVR	26	9.1 ± 4.4	0.13 ± 0.59	(−) 0.02 ± 0.08*	0.14 ± 0.76*	0	1
	ETR	11	14.6 ± 7.0	(−) 0.07 ± 0.14	0.51 ± 1.04	0.07 ± 1.50	0	0
	NR	23	7.4 ± 2.0	0.01 ± 0.30	0.09 ± 0.30	(−) 0.18 ± 0.32	0	0
Non-IFN-treated patients		98	8.2 ± 8.2	(−) 0.80 ± 0.82	0.15 ± 0.15	(−) 0.94 ± 0.95	6	2
All		158	8.7 ± 4.7	(−) 0.45 ± 2.93	0.13 ± 0.52	(−) 0.59 ± 3.78	6	3

*$P < 0.05$ versus patients without IFN treatment.
†⊿Albumin: changes in albumin concentration (g/dL)/observation period (years).
‡⊿Bilirubin: changes in bilirubin concentration (mg/dL)/observation period (years).
§⊿Platelet: changes in platelet count ($\times 10^4$/μL)/observation period (years).
ETR, end of treatment virological response; HCC, hepatocellular carcinoma; HCV, hepatitis C virus; HIV, human immunodeficiency virus; IFN, interferon; NR, no virological response; SVR, sustained virological response.

Table 5 Changes in clinical parameters and HAART in HIV–HCV co-infected patients

	Number	Age	Sex (M : F)	Observation period (years)	⊿Albumin†	⊿Bilirubin‡	⊿Platelet§	IFN	Ascites/ encephalopathy	HCC
HAART (+)	234	37.8 ± 10.4	227:7	8.4 ± 4.2	(−) 0.002 ± 0.18	0.13 ± 0.53	(−) 0.40 ± 3.71	143 (61.1%)	6	5
HAART (−)	58	38.1 ± 10.5	58:0	9.8 ± 6.0	(−) 0.14 ± 0.18	0.03 ± 0.25	(−) 1.40 ± 3.30	30 (51.7%)	3	2

†⊿Albumin: changes in albumin concentration (g/dL)/observation period (years).
‡⊿Bilirubin: changes in bilirubin concentration (mg/dL)/observation period (years).
§⊿Platelet: changes in platelet count ($\times 10^4$/[L)/observation period (years).
HAART, highly active anti-retroviral therapy; HCC, hepatocellular carcinoma; HCV, hepatitis C virus; HIV, human immunodeficiency virus.

of ribavirin/IFN combination therapy in HIV–HCV co-infected patients in this study.

The response rate to ribavirin/IFN combination therapy was 31.4% in total, and 15.3% in patients with HCV genotype 1, which are comparable rates to those achieved in previous studies on HIV–HCV co-infected patients in Western countries.[7] The low response rate in HIV–HCV co-infected patients compared with HCV mono-infected patients[12] may be attributed to several factors: impaired immune response, high HCV loads and viral quasi-species caused by frequent chances of transmission. Of these, high viral loads may be essential, because Table 2 shows that patients with genotype 1 HCV achieved SVR even by IFN monotherapy if their viral loads were low. In the era of IFN monotherapy, patients with favorable conditions were treated first of all: pretreatment viral loads in patients who received IFN monotherapy were lower than those who received PEG-IFN–ribavirin combination therapy. This may be the reason why the efficacy of PEG-IFN–ribavirin combination therapy was lower than that with IFN monotherapy in this study.

The serum bilirubin concentrations and platelet counts were improved in the patients who achieved SVR by IFN treatment. Although the response rate to IFN treatment is lower in HIV–HCV co-infected patients than in HCV mono-infected patients, the overall benefit of IFN treatment on liver function may be similarly expected in the patients who achieved SVR. HAART showed no impact on the liver function in HIV–HCV co-infected patients. Improvement of liver function can be expected only in IFN-treated patients, although there is a possibility that only patients with preserved liver function were able to receive IFN treatment. Given that liver disease is the major life-threatening factor in HIV-infected patients, IFN treatment should be considered in the early stage of HIV–HCV co-infection.

It should be noted that nine patients had hepatic decompensation and seven had HCC, and the average age of such patients was much younger than that of HCV mono-infected patients with the same complications.[9] This finding is compatible with reports from Western countries showing a faster progression of fibrosis[13] and earlier development of HCC.[14] A possibly interesting finding is that five patients (approximately 3% of patients whose serum HCV-RNA level was serially determined) cleared HCV-RNA from the serum without IFN treatment. Previous reports showed that some HIV-infected patients could spontaneously clear HCV-RNA.[15–17] The clearance of HCV among patients with chronic HCV infection is rare, although it has been

reported in Japan.[18] Three of the five patients had high HCV loads and low $CD4^+$ T-lymphocyte counts, which are generally thought to be unfavorable for spontaneous HCV clearance. A difference in immune status of HIV-infected patients from HCV mono-infected patients may be involved in such an observation, although further studies are awaited.

In summary, our study demonstrated that approximately 20% of HIV-infected patients are co-infected with HCV. Some of the HIV–HCV co-infected patients had advanced liver disease such as ascites, encephalopathy or HCC at a younger age than HCV mono-infected patients, suggesting that the progression of liver disease may be more rapid in HIV–HCV co-infected patients than in HCV-mono-infected ones. Treatments with regimens including IFN, which may improve liver function and decrease liver-related death, should be considered in HIV–HCV co-infected patients.

ACKNOWLEDGMENTS

WE THANK MS Ogawa for her assistance in the questionnaire inquiry. This work was supported in part by Health Sciences Research Grants from the Ministry of Health, Labour and Welfare of Japan (AIDS Research).

REFERENCES

1 Simon V, Ho DD, Karim QA. HIV/AIDS epidemiology, pathogenesis, prevention, and treatment. *Lancet* 2006; 368: 489–504.
2 Schneider MF, Gange SJ, Williams CM *et al.* Patterns of the hazard of death after AIDS through the evolution of antiretroviral therapy: 1984–2004. *AIDS* 2005; 19: 2009–18.
3 Kramer JR, Giordano TP, Souchek J, El-Serag HB Hepatitis C coinfection increases the risk of fulminant hepatic failure in patients with HIV in the HAART era. *J Hepatol* 2005; 42: 309–14.
4 Merchante N, Giron-Gonzalez JA, Gonzalez-Serrano M *et al.* Survival and prognostic factors of HIV-infected patients with HCV-related end-stage liver disease. *AIDS* 2006; 20: 49–57.
5 Tatsunami S, Taki M, Shirahata A, Mimaya J, Yamada K. Increasing incidence of critical liver disease among causes of death in Japanese hemophiliacs with HIV-1. *Acta Haematol* 2004; 111: 181–4.
6 Shiffman ML. Optimizing the current therapy for chronic hepatitis C virus: peginterferon and ribavirin dosing and the utility of growth factors. *Clin Liver Dis* 2008; 12: 487–505.
7 Lo Re V 3rd, Kostman JR, Amorosa VK. Management complexities of HIV/hepatitis C virus coinfection in the twenty-first century. *Clin Liver Dis* 2008; 12: 587–609.
8 Koike K, Tsukada K, Yotsuyanagi H *et al.* Prevalence of coinfection with human immunodeficiency virus and hepatitis C virus in Japan. *Hepatol Res* 2007; 37: 2–5.
9 Okita K. Clinical aspects of hepatocellular carcinoma in Japan. *Intern Med* 2006; 45: 229–33.
10 Hayashi N, Takehara T. Antiviral therapy for chronic hepatitis C: past, present, and future. *J Gastroenterol* 2006; 41: 17–27.
11 Yamaguchi T, Hashimoto S, Oka S *et al.* Physical condition and activity of daily living among HIV patients infected through blood products in Japan. *J Epidemiol* 2002; 12: 383–93.
12 Okanoue T, Itoh Y, Minami M *et al.* Guidelines for the antiviral therapy of hepatitis C virus carriers with normal serum aminotransferase based on platelet counts. *Hepatol Res* 2008; 38: 27–36.
13 Benhamou Y, Bochet M, Di Martino V *et al.* Liver fibrosis progression in human immunodeficiency virus and hepatitis C virus coinfected patients. The Multivirc Group. *Hepatology* 1999; 30: 1054–8.
14 Bräu N, Fox RK, Xiao P *et al.* Presentation and outcome of hepatocellular carcinoma in HIV-infected patients: a U.S.–Canadian multicenter study. *J Hepatol* 2007; 47: 527–37.
15 Shores NJ, Maida I, Soriano V, Nunez M. Sexual transmission is associated with spontaneous HCV clearance in HIV-infected patients. *J Hepatol* 2008; 49: 323–8.
16 Falconer K, Gonzalez VD, Reichard O, Sandberg JK, Alaeus A Spontaneous HCV clearance in HCV/HIV-1 coinfection associated with normalized CD4 counts, low level of chronic immune activation and high level of T cell function. *J Clin Virol* 2008; 41: 160–3.
17 Soriano V, Mocroft A, Rockstroh J *et al.* Spontaneous Viral Clearance, Viral Load, and Genotype Distribution of Hepatitis C Virus (HCV) in HIV-Infected Patients with Anti-HCV Antibodies in Europe. *J Infect Dis* 2008; 198: 1337–44.
18 Sugiyasu Y, Yuki N, Nagaoka T *et al.* Histological improvement of chronic liver disease after spontaneous serum hepatitis C virus clearance. *J Med Virol* 2003; 69: 41–9.

International Journal of Antimicrobial Agents 34 (2009) 347–350

Contents lists available at ScienceDirect

International Journal of Antimicrobial Agents

journal homepage: http://www.elsevier.com/locate/ijantimicag

Short communication

Analysis of plasmid-mediated multidrug resistance in *Escherichia coli* and *Klebsiella oxytoca* isolates from clinical specimens in Japan

Takashi Ode[a,*], Ryoichi Saito[b], Wakako Kumita[a], Kenya Sato[a], Shu Okugawa[b], Kyoji Moriya[b], Kazuhiko Koike[b], Noboru Okamura[a]

[a] *Department of Microbiology and Immunology, Graduate School of Health Sciences, Tokyo Medical and Dental University, 1-5-45 Yushima, Bunkyo-ku, Tokyo 113-8510, Japan*
[b] *Department of Infection Control and Prevention, The University of Tokyo Hospital, 7-3-1 Hongo, Bunkyo-ku, Tokyo 113-8655, Japan*

ARTICLE INFO

Article history:
Received 19 March 2009
Accepted 18 May 2009

Keywords:
qnr
Aminoglycoside acetyltransferase
Extended-spectrum β-lactamase
Metallo-β-lactamase
Class 1 integron

ABSTRACT

This study investigated the relationship of plasmid-mediated quinolone resistance (PMQR) and aminoglycoside resistance among oxyimino-cephalosporin-resistant *Escherichia coli* ($n = 46$) and *Klebsiella oxytoca* ($n = 28$) clinical isolates in Japan. Seventy-three isolates appeared to produce an extended-spectrum β-lactamase (ESBL) and one *K. oxytoca* isolate produced IMP-1 metallo-β-lactamase (MBL). Polymerase chain reaction (PCR) and sequencing confirmed that eight CTX-M-9/SHV-12-producing isolates, one IMP-1-producing *K. oxytoca* isolate, and six ESBL-positive *E. coli* isolates respectively possessed PMQR genes *qnrA1*, *qnrB6*, and *aac(6′)-Ib-cr*. All *qnr*-positive isolates also carried either *aac(6′)-Ib* or *aac(6′)-IIc* aminoglycoside acetyltransferase genes. Resistance determinants to β-lactams, quinolones and aminoglycosides were co-transferred with a plasmid of ca. 140 kb. The *qnrA1* gene was located downstream of insertion sequence ISCR1 in complex class 1 integrons. A novel *qnrA1*-carrying class 1 integron with the cassette arrangement *aac(6′)-IIc–aadA2* as well as a unique class 1 integron with bla_{IMP-1}*–aac(6′)-IIc* cassettes on the plasmid carrying *qnrB6* were found in *K. oxytoca* isolates. We describe the identification of *qnrB6* and *aac(6′)-Ib-cr* and the close association of *qnr* with *aac(6′)-Ib* and *aac(6′)-IIc* for the first time in clinical isolates producing ESBL or MBL in Japan.

1. Introduction

Quinolone resistance is usually caused by chromosomal mutations, however the plasmid-mediated quinolone resistance (PMQR) determinants QnrA, QnrB, QnrS and AAC(6′)-Ib-cr have been described [1]. Although these PMQR determinants result in low-level quinolone resistance, such reduced susceptibility is important because it facilitates the selection of mutants with higher-level resistance. In Japan, although *qnrS* was first found in *Shigella flexneri* [2] and *qnrA* was also described in Enterobacteriaceae clinical isolates [3,4], the presence of clinical strains harbouring *qnrB* or *aac(6′)-Ib-cr* has not been reported. Furthermore, a recent prevalence study of *qnr* and the *qepA* plasmid-mediated efflux pump gene suggested a low prevalence of *Escherichia coli* harbouring *qepA* or *qnr* in Japan [5].

Many studies have shown that most *qnrA*-positive enterobacterial isolates are associated with plasmid-mediated AmpC-type β-lactamases, extended-spectrum β-lactamases (ESBLs) and metallo-β-lactamases (MBLs) [1,3,4,6,7]. *qnrA* is often located in complex class 1 integrons between common region 1 (CR1), comprising orf513 recombinase and a second copy of the 3′ conserved segment (3′-CS2), together with other resistance gene cassettes such as trimethoprim and aminoglycoside resistance cassettes [1]. However, little has been reported on the genetic context of *qnr* in Japan.

The present study was conducted to investigate the genetic relationship of the PMQR genes *qnr* and *aac(6′)-Ib-cr* as well as the 6′-*N*-aminoglycoside acetyltransferase [AAC(6′)] genes *aac(6′)-Ib* and *aac(6′)-IIc* among oxyimino-cephalosporin-resistant *E. coli* and *Klebsiella oxytoca* clinical isolates in Japan and to determine the structure of class 1 integrons, including the insertion sequence CR1 (ISCR1) element associated with *qnr*.

2. Materials and methods

2.1. Bacterial strains

A total of 46 *E. coli* and 28 *K. oxytoca* clinical isolates resistant to one or more of cefotaxime, ceftazidime and aztreonam, collected at the University of Tokyo Hospital (Tokyo, Japan) between November 2005 and October 2006, were examined in this study.

* Corresponding author. Tel.: +81 3 5803 4515; fax: +81 3 5803 5375.
E-mail addresses: takashi.ode.mt@gmail.com, takashi.0630@jcom.home.ne.jp (T. Ode).

0924-8579/$ – see front matter © 2009 Elsevier B.V. and the International Society of Chemotherapy. All rights reserved.
doi:10.1016/j.ijantimicag.2009.05.007

2.2. Susceptibility testing

ESBL and MBL production was confirmed by double-disk synergy tests using clavulanic acid and ethylene diamine tetra-acetic acid (EDTA) as β-lactamase inhibitors, respectively. Minimum inhibitory concentrations (MICs) of amikacin, aztreonam, cefazolin, cefoperazone, cefotaxime, ceftazidime, ciprofloxacin, gentamicin, imipenem, levofloxacin and meropenem were determined by the broth microdilution method according to the Clinical and Laboratory Standards Institute [8]. Etest (AB BIODISK, Solna, Sweden) was used to detect low-level reduction in ciprofloxacin and levofloxacin susceptibility. Quality control for the MICs was performed using the reference strains *Staphylococcus aureus* ATCC 21293, *E. coli* ATCC 25922 and *Pseudomonas aeruginosa* ATCC 27853.

2.3. Polymerase chain reaction (PCR) and sequencing

PCR amplification was performed with Premix *Taq* enzyme (Takara Bio, Shiga, Japan) according to the manufacturer's instructions. Both strands of the purified PCR fragments were sequenced with an ABI PRISM 3130 DNA sequencer (Applied Biosystems, Foster City, CA) and a similarity search was conducted using the BLAST program (DDBJ, Shizuoka, Japan).

2.4. Characterisation of β-lactamases

The bla_{TEM}, bla_{SHV} and bla_{CTX-M} genes were amplified using the published primers [9,10]. The presence of MBL genes bla_{IMP} and bla_{VIM} was tested with type-specific primers described previously [11]. For all *qnr*-positive isolates, the nucleotide sequences of the *bla* genes were determined by sequencing.

2.5. Detection of the plasmid-mediated quinolone resistance determinants and the AAC(6′) genes

Screening for *qnrA*, *qnrB* and *qnrS* was carried out by multiplex PCR amplification as described previously [12]. Sequences of *qnrA* and *qnrB* were determined by PCR sequencing with primers 5′-TTGATAAAGTTTTTCAGCAA and 5′-CTAATCCGGCAGCACTATTA for *qnrA1* and primers 5′-ATGACGCCATTACTGTAT and 5′-CTAACCAATCACCGCGAT for *qnrB6*, designed to amplify a 647-bp fragment and a 681-bp fragment, respectively. The presence of *aac(6′)-Ib* and *aac(6′)-Ib-cr* variant was determined by PCR sequencing using a common primer pair [13]. The primer pair used for detection of *aac(6′)-IIc* was 5′-CCAACAATGCCGCAATAGTT and 5′-ATGACCACTTCCCCTTGATT, amplifying a 573-bp fragment, designed in the present study.

2.6. Conjugation experiments and extraction of plasmids

Conjugation experiments were performed in Luria–Bertani broth with nine *qnr*-positive clinical isolates as donors and an *E. coli* C600 strain as recipient. Transconjugant clones were selected on Drigalski agar (BTB agar) plates containing 100 mg/L rifampicin and 4 mg/L cefotaxime (or 0.03 mg/L ciprofloxacin in the absence of transfer with cefotaxime). Plasmid DNA was extracted from donors and transconjugants using a NucleoBond® Xtra Midi (Macherey-Nagel, Düren, Germany) according to the manufacturer's instructions and was subjected to electrophoresis on 0.7% (w/v) agarose (Takara Bio) gel with ethidium bromide at 50 V for 3 h. The size of transferred plasmids was estimated by adding up EcoRI and NotI restriction fragments.

2.7. Analysis of the genetic environment of qnr and class 1 integron structures

The genetic context of the *qnr* genes was investigated by PCR mapping and subsequent sequencing as described previously [14]. The content and order of the gene cassettes inserted between the 5′ conserved segment (5′-CS) and 3′-CS1 were determined by sequencing as described previously [15]. Finally, the regions between *intI1* in 5′-CS and a second copy of *qacEΔ1* in 3′-CS2 were sequenced using a primer walking strategy.

Table 1
Antibiotic resistance genes and susceptibility profiles in donors (*qnr*-positive isolates), the *Escherichia coli* recipient and transconjugants.

Strain	Genotype of			Cassette array[a]	MIC (mg/L)										
	Qnr	β-Lactamase	AAC(6′)		CIP	LVX	CFZ	CFP	CTX	CAZ	ATM	IPM	MEM	GEN	AMK
Escherichia coli (donors)															
E5	*qnrA1*	bla_{TEM-1}, $bla_{CTX-M-9}$	*aac(6′)-Ib*	[*aadB–aadA2*]	>64	32	>128	>128	16	<1	2	≤1	≤1	>128	32
E15	*qnrA1*	bla_{SHV-12}	*aac(6′)-Ib*	[*dfr16–aadA2*]	≤0.5	≤0.5	>128	32	32	>64	>64	≤1	≤1	≤2	8
E18	*qnrA1*	bla_{SHV-12}	*aac(6′)-Ib*	[*dfr16–aadA2*]	≤0.5	≤0.5	>128	16	8	>64	>64	≤1	≤1	≤2	8
Klebsiella oxytoca (donors)															
K5	*qnrA1*	bla_{TEM-1}, $bla_{CTX-M-9}$	*aac(6′)-IIc*	[*aadB–aadA2*]	≤0.5	≤0.5	>128	64	8	≤1	4	≤1	≤1	8	≤2
K7	*qnrA1*	$bla_{CTX-M-9}$	*aac(6′)-Ib*	[*aadB–aadA2*]	≤0.5	≤0.5	>128	>128	8	2	>64	≤1	≤1	8	8
K9	*qnrA1*	bla_{TEM-1}, $bla_{CTX-M-9}$	*aac(6′)-IIc*[b]	[*aac(6′)-IIc–aadA2*]	≤0.5	2	>128	64	8	2	8	≤1	≤1	8	≤2
K10	*qnrA1*	bla_{TEM-1}, $bla_{CTX-M-9}$	*aac(6′)-IIc*	[*aadB–aadA2*]	≤0.5	2	>128	64	8	≤1	4	≤1	≤1	4	≤2
K16	*qnrA1*	bla_{TEM-1}, $bla_{CTX-M-9}$	*aac(6′)-IIc*	[*aadB–aadA2*]	≤0.5	2	>128	64	4	≤1	4	≤1	≤1	8	≤2
K27	*qnrB6*	bla_{IMP-1}[b]	*aac(6′)-IIc*[b]	[bla_{IMP-1}–*aac(6′)-IIc*]	1	2	>128	>128	32	>64	≤1	2	4	≤1	≤2
E. coli C600 (recipient)					0.016	0.032	≤2	≤8	≤1	≤1	≤1	≤1	≤1	≤1	≤2
Transconjugants[c]															
E5TC-cip	*qnrA1*	bla_{TEM-1}, $bla_{CTX-M-9}$	*aac(6′)-Ib*	[*aadB–aadA2*]	0.25	0.25	N.T.	N.T.	8	≤1	≤1	≤1	≤1	64	32
E15TC-cip	*qnrA1*	bla_{SHV-12}	*aac(6′)-Ib*	[*dfr16–aadA2*]	0.25	0.25	N.T.	N.T.	32	32	64	≤1	≤1	≤1	16
E18TC-cip	*qnrA1*	bla_{SHV-12}	*aac(6′)-Ib*	[*dfr16–aadA2*]	0.125	0.125	N.T.	N.T.	8	16	>64	≤1	≤1	≤1	8
K5TC-ctx	N.D.	bla_{TEM-1}, $bla_{CTX-M-9}$	*aac(6′)-IIc*	N.D.	0.016	0.016	>32	>32	16	≤1	>16	≤1	≤1	8	≤2
K9TC-ctx	*qnrA1*	bla_{TEM-1}, $bla_{CTX-M-9}$	*aac(6′)-IIc*[b]	[*aac(6′)-IIc–aadA2*]	0.25	0.25	>32	>32	32	≤1	>16	≤1	≤1	>8	≤2
K10TC-ctx	*qnrA1*	bla_{TEM-1}, $bla_{CTX-M-9}$	*aac(6′)-IIc*	[*aadB–aadA2*]	0.25	0.125	>32	>32	16	≤1	8	≤1	≤1	4	≤2
K16TC-ctx	N.D.	bla_{TEM-1}, $bla_{CTX-M-9}$	N.D.	N.D.	0.016	0.016	>32	>32	16	≤1	>16	≤1	≤1	≤1	≤2
K16TC-cip	*qnrA1*	bla_{TEM-1}, $bla_{CTX-M-9}$	*aac(6′)-IIc*	[*aadB–aadA2*]	0.25	0.25	N.T.	N.T.	32	≤1	4	≤1	≤1	8	4
K27TC-ctx	*qnrB6*	bla_{IMP-1}[b]	*aac(6′)-IIc*[b]	[bla_{IMP-1}–*aac(6′)-IIc*]	0.125	0.25	N.T.	N.T.	>16	>64	≤1	2	4	≤1	2

MIC, minimum inhibitory concentration; CIP, ciprofloxacin; LVX, levofloxacin; CFZ, cefazolin; CFP, cefoperazone; CTX, cefotaxime; CAZ, ceftazidime; ATM, aztreonam; IPM, imipenem; MEM, meropenem; GEN, gentamicin; AMK, amikacin; N.T., not tested; N.D., not detected.

[a] Gene cassette array in class 1 integrons.

[b] Genes carried as cassettes by the class 1 integrons.

[c] cip, transconjugants selected by ciprofloxacin; ctx, transconjugants selected by cefotaxime.

2.8. Nucleotide sequence accession numbers

Nucleotide sequence data of integrons InK9AT and InK27AT are available in the DDBJ/EMBL/GenBank databases under the accession numbers AB469045 and AB469046, respectively.

3. Results and discussion

The phenotypic tests revealed that 46 *E. coli* and 27 *K. oxytoca* oxyimino-cephalosporin-resistant clinical isolates produced ESBLs. Only one *K. oxytoca* isolate appeared to produce an MBL. Of these β-lactamase producers, 28 *E. coli* and 16 *K. oxytoca* isolates showed resistance to ciprofloxacin and 18 *E. coli* and 12 *K. oxytoca* isolates showed susceptibility to ciprofloxacin.

The bla_{CTX-M} gene was amplified by PCR in 60 (82.2%) of the 73 ESBL producers, including the combination of bla_{TEM} and bla_{CTX-M} in *E. coli* isolates (43.5%; 20/46) and the combination of bla_{SHV} and bla_{CTX-M} in *K. oxytoca* isolates (44.4%; 12/27). The bla_{IMP} gene was detected in one MBL-producing *K. oxytoca* isolate. The bla_{VIM} gene was not observed, and no *bla* genes were detected in five *E. coli* isolates.

For the PMQR genes, *qnrA* was detected in 3 (6.5%) of 46 *E. coli* and 5 (18.5%) of 27 *K. oxytoca* isolates that produced ESBLs, and *qnrB* was detected in 1 *K. oxytoca* isolate producing MBL. The presence of *qnrS* was not observed. The sequences of *qnrA* and *qnrB* were identical to those of *qnrA1* and *qnrB6*, respectively. Of the nine *qnr*-positive isolates, one *E. coli* isolate E5 demonstrated higher resistance to ciprofloxacin (MIC > 64 mg/L), whereas the other eight isolates were susceptible to ciprofloxacin (MIC ≤ 0.5 or 1 mg/L) (Table 1).

The *aac(6′)-Ib-cr* gene was detected in 6 *E. coli* isolates (13.0%) that were resistant to ciprofloxacin (MIC > 64 mg/L), but was not detected in any *K. oxytoca* isolate. These six isolates were positive for bla_{CTX-M}, including two isolates also positive for bla_{TEM}, and this is the first report of *aac(6′)-Ib-cr* identified from the clinical setting in Japan. No isolates possessing *qnr* and *aac(6′)-Ib-cr* in combination were present, suggesting that these two genes have no relationship as described previously in Enterobacteriaceae from the USA [13].

The presence of the *aac(6′)-Ib* gene, responsible for resistance to amikacin, was confirmed in 4 of 9 *qnr*-positive isolates and 1 of 65 *qnr*-negative isolates (amikacin MIC range 8–32 mg/L). The *aac(6′)-IIc* gene, responsible for resistance to gentamicin, was detected in 6 *K. oxytoca* isolates (gentamicin MIC range 4–8 mg/L, except for ≤1 mg/L in isolate K27), comprising 5 of 9 *qnr*-positive isolates and 1 of 65 *qnr*-negative isolates. In the present study, the observation of the *aac(6′)-IIc* cassette prompted us to screen all the isolates for this gene. The results demonstrated that the *aac(6′)-IIc* gene was more prevalent among *qnr*-positive *K. oxytoca* isolates than among all *qnr*-negative isolates (5 of 6 isolates versus 1 of 65 isolates), whilst the *aac(6′)-IIc* gene has been uncommon worldwide, especially in Asia.

All *qnr*-positive isolates possessed combinations of three or more antibiotic resistance genes responsible for resistance to β-lactams, quinolones or aminoglycosides (Table 1). Six isolates carried the $bla_{CTX-M-9}$ ESBL gene, of which five isolates also carried bla_{TEM-1} encoding narrow-spectrum β-lactamase (cefotaxime MIC range 4–16 mg/L). Two *E. coli* isolates harboured the bla_{SHV-12} ESBL gene (ceftazidime MIC > 64 mg/L). The bla_{IMP} allele detected in one phenotypically MBL-positive isolate was identified as bla_{IMP-1}, conferring reduced susceptibility to imipenem and meropenem (MICs 2 mg/L and 4 mg/L, respectively).

The *qnr* genes were transferred from seven clinical isolates (E5, E15, E18, K9, K10, K16, and K27) to their transconjugants (Table 1). The *qnr*-containing transconjugants (K9TC-ctx, K10TC-ctx and K27TC-ctx selected by cefotaxime, and E5TC-cip, E15TC-cip, E18TC-cip and K16TC-cip selected by ciprofloxacin) conferred decreased susceptibility to ciprofloxacin (MIC range 0.125–0.25 mg/L) and levofloxacin (MIC range 0.125–0.25 mg/L), representing 8–16-fold and 4–8-fold increases compared with those of the recipient (MICs of 0.016 mg/L and 0.032 mg/L), respectively. Resistance or reduced susceptibility to β-lactams and aminoglycosides was co-transferred with the *bla* genes and the *aac(6′)* genes carried by donors, respectively. Two *qnr*-negative transconjugants were selected using cefotaxime; bla_{TEM-1}, $bla_{CTX-M-9}$ and *aac(6′)-IIc* were transferred to K5TC-ctx, and bla_{TEM-1} and $bla_{CTX-M-9}$ were transferred to K16TC-ctx. Single plasmids were transferred with or without *qnr* to all transconjugants and their sizes were estimated to be ca. 140 kb. Of these, two representative plasmids in K9TC-ctx and K27TC-ctx were designated pK9AT and pK27AT, respectively.

In the present study, β-lactamase producers frequently possessed the PMQR determinants (20.3%), the AAC(6′) genes (14.9%) or both (12.2%). Further striking features of the present study are the first findings showing that *qnrB6* was carried by an IMP-1 MBL-producing *K. oxytoca* isolate on the same plasmid, and that *qnr*-positive isolates also carried either *aac(6′)-Ib* or *aac(6′)-IIc* on the same plasmid. On the other hand, the linkage of IMP-1 and *qnrB2* in Taiwan [6] and the linkage of VIM-1, *qnrS1* and *aac(6′)-Ib* in Italy [7] have been reported. Our results demonstrating that *aac(6′)-Ib* and *aac(6′)-IIc* were predominant in *qnr*-positive isolates (100%; 9/9) compared with *qnr*-negative isolates (3.1%; 2/65) suggest the genetically close association of quinolone resistance with aminoglycoside resistance.

qnr-positive isolates and their transconjugants carried several types of gene cassettes between 5′-CS and 3′-CS1 (Table 1), and *qnrA1* was located between *orf513* and *ampR*. The complex class 1 integron structure on the plasmids from two *E. coli* isolates was identical to that of In36 (GenBank accession no. AY259085) containing the *dfr16* cassette followed by the *aadA2* cassette.

The structure containing the *aadB* cassette located upstream of the *aadA2* cassette, observed on plasmids from one *E. coli* and four *K. oxytoca* isolates, was similar to that of InKp760 (GenBank accession no. AJ971341), with the replacement of *ampC* with *qnrA1*.

Furthermore, two unique class 1 integrons were found on pK9AT and pK27AT, designated InK9AT and InK27AT, respectively. InK9AT was a novel complex class 1 integron that contained the *aac(6′)-IIc* cassette followed by the *aadA2* cassette, whose structure was also similar to In36 with the replacement of the *dfr16* cassette with the *aac(6′)-IIc* cassette. On the other hand, the bla_{IMP-1} cassette was inserted upstream of the *aac(6′)-IIc* cassette in InK27AT. This structure was similar to In87 (GenBank accession no. AY648125) carrying the bla_{VIM-1} cassette followed by the *aac(6′)-IIc* cassette. The InK9AT cassette arrangement is described for the first time in the present study and we have shown the first identification of the InK27AT cassette arrangement from a *K. oxytoca* clinical isolate and its linkage of *qnrB6* on a single plasmid.

From two unique integrons, two versions of the P_c promoter (formerly P_{ant} or P1) responsible for expression of cassette genes were found in 5′-CS, which were the strong version of P_c (TTGACA–17 bp–TAAACT) found in InK9AT and the weak version of P_c (TGGACA–17 bp–TAAGCT) found in InK27AT. A potential secondary promoter P2 was inactive (TTGTTA–14 bp–TACAGT) in both integrons, although P2 potentially becomes a strong promoter due to insertion of 3 bp into the spacer region. These observations strongly suggest that the different levels of resistance to gentamicin in our transconjugant strains carrying pK9AT and pK27AT (MIC > 8 mg/L for pK9AT versus MIC ≤ 1 mg/L for pK27AT) are affected by different levels of *aac(6′)-IIc* expression owing to the different versions of P_c promoters or the position of the cassette.

The genetic context of *qnrA1* (*orf513–qnrA1–ampR–qacEΔ1*) was conserved among all *qnrA1*-carrying plasmids and was identical to that of In36 and that described in Japan [3], although repeated

attempts to amplify the surrounding regions of *qnrB6* on pK27AT were unsuccessful. In contrast, the cassette content and order within the variable region between 5′-CS and 3′-CS1 on all *qnr*-carrying plasmids have variety. These observations suggest that *qnr*-carrying plasmids have been disseminated with the conserved ISCR1 element and have acquired genetic variety by IntI1-mediated mobilisation of the gene cassettes.

In conclusion, the present study demonstrated the relatively high prevalence of PMQR determinants among ESBL- or MBL-producing isolates in Japan, and two unique integrons were identified on the plasmid carrying the *qnr* genes. Moreover, identification of *qnrB6* and *aac(6′)-Ib-cr*, and close association of *qnr* with *aac(6′)-Ib* and *aac(6′)-IIc*, are described for the first time in clinical isolates producing ESBL or MBL in Japan. The emergence of integrons with novel gene cassettes and plasmid-mediated resistance genes as well as the spread of ISCR1 elements are serious considerations in further dissemination of various resistance genes.

Acknowledgments

The authors thank N. Tajitsu and M. Sakoda for technical assistance in this study.

Funding: The research activity of RS was supported by Grants-in-Aid for Scientific Research from the Japan Society for the Promotion of Science (grant 20930009).

Competing interests: None declared.

Ethical approval: Not required.

References

[1] Robicsek A, Jacoby GA, Hooper DC. The worldwide emergence of plasmid-mediated quinolone resistance. Lancet Infect Dis 2006;6:629–40.

[2] Hata M, Suzuki M, Matsumoto M, Takahashi M, Sato K, Ibe S, et al. Cloning of a novel gene for quinolone resistance from a transferable plasmid in *Shigella flexneri* 2b. Antimicrob Agents Chemother 2005;49:801–3.

[3] Saga T, Akasaka T, Takase H, Tanaka M, Sato K, Kaku M. First detection of the plasmid-mediated quinolone resistance determinant *qnrA* in Enterobacteriaceae clinical isolates in Japan. Int J Antimicrob Agents 2007;29:738–9.

[4] Saito R, Kumita W, Sato K, Chida T, Okamura N, Moriya K, et al. Detection of plasmid-mediated quinolone resistance associated with *qnrA* in an *Escherichia coli* clinical isolate producing CTX-M-9 β-lactamase in Japan. Int J Antimicrob Agents 2007;29:600–2.

[5] Yamane K, Wachino J, Suzuki S, Arakawa Y. Plasmid-mediated *qepA* gene among *Escherichia coli* clinical isolates from Japan. Antimicrob Agents Chemother 2008;52:1564–6.

[6] Wu JJ, Ko WC, Tsai SH, Yan JJ. Prevalence of plasmid-mediated quinolone resistance determinants QnrA, QnrB, and QnrS among clinical isolates of *Enterobacter cloacae* in a Taiwanese hospital. Antimicrob Agents Chemother 2007;51:1223–7.

[7] Aschbacher R, Doumith M, Livermore DM, Larcher C, Woodford N. Linkage of acquired quinolone resistance (*qnrS1*) and metallo-β-lactamase (bla_{VIM-1}) genes in multiple species of Enterobacteriaceae from Bolzano, Italy. J Antimicrob Chemother 2008;61:515–23.

[8] Clinical and Laboratory Standards Institute. Performance standards for antimicrobial susceptibility testing. Fifteenth informational supplement. Document M100-S15. Wayne, PA: CLSI; 2005.

[9] Yagi T, Kurokawa H, Shibata N, Shibayama K, Arakawa Y. A preliminary survey of extended-spectrum β-lactamases (ESBLs) in clinical isolates of *Klebsiella pneumoniae* and *Escherichia coli* in Japan. FEMS Microbiol Lett 2000;184:53–6.

[10] Saladin M, Cao VT, Lambert T, Donay JL, Herrmann JL, Ould-Hocine Z, et al. Diversity of CTX-M β-lactamases and their promoter regions from Enterobacteriaceae isolated in three Parisian hospitals. FEMS Microbiol Lett 2002;209:161–8.

[11] Shibata N, Doi Y, Yamane K, Yagi T, Kurokawa H, Shibayama K, et al. PCR typing of genetic determinants for metallo-β-lactamases and integrases carried by Gram-negative bacteria isolated in Japan, with focus on the class 3 integron. J Clin Microbiol 2003;41:5407–13.

[12] Robicsek A, Strahilevitz J, Sahm DF, Jacoby GA, Hooper DC. *qnr* prevalence in ceftazidime-resistant Enterobacteriaceae isolates from the United States. Antimicrob Agents Chemother 2006;50:2872–4.

[13] Park CH, Robicsek A, Jacoby GA, Sahm D, Hooper DC. Prevalence in the United States of *aac(6′)-Ib-cr* encoding a ciprofloxacin-modifying enzyme. Antimicrob Agents Chemother 2006;50:3953–5.

[14] Cambau E, Lascols C, Sougakoff W, Bébéar C, Bonnet R, Cavallo JD, et al. Occurrence of *qnrA*-positive clinical isolates in French teaching hospitals during 2002–2005. Clin Microbiol Infect 2006;12:1013–20.

[15] Lévesque C, Piché L, Larose C, Roy PH. PCR mapping of integrons reveals several novel combinations of resistance genes. Antimicrob Agents Chemother 1995;39:185–91.

Proteomics Analysis of Mitochondrial Proteins Reveals Overexpression of a Mitochondrial Protein Chaperon, Prohibitin, in Cells Expressing Hepatitis C Virus Core Protein

Takeya Tsutsumi,[1] Mami Matsuda,[2] Hideki Aizaki,[2] Kyoji Moriya,[1] Hideyuki Miyoshi,[1] Hajime Fujie,[1] Yoshizumi Shintani,[1] Hiroshi Yotsuyanagi,[1] Tatsuo Miyamura,[2] Tetsuro Suzuki,[2] and Kazuhiko Koike[1]

The hepatitis C virus (HCV) core protein is involved in viral pathogenesis such as oxidative stress induction and lipid metabolism disturbance, and is primarily located in the cytoplasm and endoplasmic reticulum in association with lipid droplets as well as in the mitochondria. To clarify the impact of the core protein on mitochondria, we analyzed the expression pattern of mitochondrial proteins in core protein-expressing cells by two-dimensional polyacrylamide gel electrophoresis. Several proteins related to the mitochondrial respiratory chain or protein chaperons were identified by mass spectrometry. Among the identified proteins with consistently different expressions, prohibitin, a mitochondrial protein chaperon, was up-regulated not only in core-expressing cells but also in full-genomic replicon cells and livers of core-gene transgenic mice. The stability of prohibitin was increased through interaction with the core protein. Further analysis demonstrated that interaction of prohibitin with mitochondrial DNA-encoded subunits of cytochrome c oxidase (COX) was disturbed by the core protein, resulting in a significant decrease in COX activity. *Conclusion:* The HCV core protein affects the steady-state levels of a subset of mitochondrial proteins including prohibitin, which may lead to an impaired function of the mitochondrial respiratory chain with the overproduction of oxidative stress. (HEPATOLOGY 2009;50:378-386.)

The hepatitis C virus (HCV) is a causative agent of chronic hepatitis, which often leads to cirrhosis and, eventually, to the development of hepatocellular carcinoma (HCC). However, the mechanism of hepatocarcinogenesis in HCV infection is not yet fully elucidated. The HCV core protein forms the viral nucleocapsid protein and has various properties that modulate cellular processes in numerous ways. The core protein binds to cellular proteins, suppresses or enhances apoptosis, and modulates the transcription of some host genes.[1] In addition, transgenic mice expressing the core protein develop HCC,[2-4] indicating a direct contribution of the core protein to the pathogenesis of hepatitis C.

The core protein is mostly localized to the endoplasmic reticulum (ER), but we and other groups have shown its localization to the mitochondria in cultured cells and transgenic mice.[2,5,6] In addition, the double structure of mitochondrial membranes is disrupted in hepatocytes of core-gene transgenic mice.[2-4] Evidence suggests that the core protein modulates some mitochondrial functions, including fatty acid β-oxidation, the impairment of which may induce lipid abnormalities and hepatic steatosis. In addition, the mitochondrion is an important source of reactive oxygen species (ROS). In livers of transgenic

Abbreviations: 2D-PAGE, two-dimensional polyacrylamide gel electrophoresis; COX, cytochrome c oxidase; ER, endoplasmic reticulum; Ero1, ER protein endoplasmic oxidoreduction-1; HCC, hepatocellular carcinoma; HCV, hepatitis C virus; HSP, heat shock protein; IFN, interferon; MnSOD, manganese superoxide dismutase; NS, nonstructural; OST48, oligosaccharyltransferases-48; PDH, pyruvate dehydrogenase; PDI, protein disulfide isomerase; ROS, reactive oxygen species; TFA, trifluoroacetic acid.

From the [1]Department of Internal Medicine, Graduate School of Medicine, University of Tokyo; [2]Department of Virology II, National Institute of Infectious Diseases, Tokyo, Japan.

Received June 17, 2008; accepted March 20, 2009.

Supported by a grant-in-aid for Scientific Research from the Japan Society for the Promotion of Science, from the Ministry of Health, Labour and Welfare of Japan (Research on Hepatitis), from the Ministry of Education, Culture, Sports, Science and Technology (Priority Area), from The Sankyo Foundation of Life Science, and from The Charitable Trust Araki Memorial Promotion Fund. T. T. is an awardee of the Research Resident Fellowship from the Viral Hepatitis Research Foundation of Japan.

Address reprint requests to: Kazuhiko Koike, M.D., Ph.D., Department of Gastroenterology, Internal Medicine, Graduate School of Medicine, University of Tokyo, 7-3-1 Hongo, Bunkyo-ku, Tokyo 113-8655, Japan. E-mail: kkoike-tky@umin.ac.jp; fax: (81) 3-5800-8799

Published online in Wiley InterScience (www.interscience.wiley.com).

DOI 10.1002/hep.22998

Potential conflict of interest: Nothing to report.

Additional Supporting Information may be found in the online version of this article.

mice harboring the core gene, increased ROS production has been observed.[7-9] A recent study found, by the proteomic profiling of biopsy specimens, that an impairment in key mitochondrial processes, including fatty acid oxidation and oxidative phosphorylation, and in the response to oxidative stress occurs in HCV-infected human liver with advanced fibrosis.[10] Therefore, it is probable that the HCV core protein affects mitochondrial functions because such pathogenesis is observed in both HCV core-transgenic mice and HCV-infected patients.[11-13]

The recent progress in proteomics has opened new avenues for disease-related biomarker discovery. Among proteomics approaches, two-dimensional polyacrylamide gel electrophoresis (2D-PAGE) is a technique for the separation and identification of proteins in a sample by displacement in two dimensions oriented at right angles to one another. This method is generally used as a component of proteomics and is the step used for the isolation of proteins for further characterization by mass spectrometry. 2D-PAGE is particularly useful when comparing two related samples such as healthy and diseased tissue. For example, proteins that are more abundant in diseased tissue may represent novel drug targets or diagnostic markers. In fact, several candidate biomarkers for many human cancers have been identified by this approach.[14] There are, however, tens of thousands of proteins in a cell, differing in abundance over six orders of magnitude. 2D-PAGE is not sensitive enough to detect rare proteins, and hence many proteins are not resolved. Therefore, splitting a sample into different fractions is often necessary to reduce the complexity of protein mixtures prior to 2D-PAGE. For this advantage, Lescuyer et al.[15] performed a 2D-PAGE of human mitochondrial proteins derived from the placenta and identified proteins mainly by peptide mass fingerprinting.

In this study, we performed a 2D-PAGE of mitochondria isolated from HepG2 cells stably expressing the HCV core protein and identified several proteins of different expressions when compared with control HepG2 cells. Among up-regulated proteins in the core-expressing cells, we focused on prohibitin, which functions as a mitochondrial protein chaperon, and found that the core protein interacts with prohibitin and represses the interaction between prohibitin and subunit proteins of cytochrome c oxidase (COX), which may lead to decreases in the expression level of the proteins and in COX activity. These results may explain the pathogenesis of liver disease in HCV infection including ROS induction.

Materials and Methods

Cells and Purification of Mitochondria. Hep39 cells,[16] which stably express the HCV core protein, and control HepG2 cells (Hepswx) were grown in Dulbecco's modified Eagle medium (DMEM) containing 10% fetal bovine serum and 1 mg/mL G418. Mitochondria were purified using Nycodenz (Nycomed Pharma, Zürich, Switzerland) according to the protocols reported by Okado-Matsumoto et al.[17] For transient transfection experiments, HepG2 cells were transfected with a core-expression plasmid using TransIT-LT1 (Mirus Bio, Madison, WI). Huh7 cells harboring HCV genotype 1b full-genomic (RCYM1)[18] or subgenomic replicon (5-15), and livers of 3-month-old core-gene transgenic mice[2] were also used for the analysis.

2D-PAGE. Gel electrophoresis in the first dimension was performed using an immobilized pH gradient gel (Immobiline Dry Strip gel, pH 4-7 linear, 13 cm; GE Healthcare, Uppsala, Sweden). The two-dimensional separation was performed on 12.5%, 14 × 16 cm^2, SDS polyacrylamide gels. After the electrophoresis, gels were silver-stained using a silver staining kit (GE Healthcare) according to the manufacturer's protocols. The stained gels were scanned and electronic images of the gels were analyzed using ImageMaster 2D Elite software (GE Healthcare).

In-Gel Digestion and Matrix-Assisted Laser Desorption Ionization, Time-of-Flight Mass Spectrometry (MALDI-TOF-MS). Protein spots on the gels were excised and a "control" piece was cut from a blank region of the gel and processed in parallel with the sample. In-gel digestion with trypsin was performed as reported.[19] The resulting peptides were concentrated using Zip-Tip C18 (Millipore, Bedford, MA). The peptide mixtures were eluted from Zip-Tip with 75% acetonitrile in 0.1% trifluoroacetic acid (TFA). The matrix (α-cyano-4-hydroxycinnamic acid dissolved in 50% acetonitrile, 0.1% TFA) was deposited on a dried sample target. Then 0.5-μL aliquots of the analyte solution were deposited onto matrix surfaces and the solvent was allowed to evaporate at ambient temperature. The digests were analyzed with a TOF mass spectrometer, PE Biosystems Voyager DE STR MALDI (Foster City, CA).

Database Analysis. For protein identification the measured monoisotopic masses of the peptides were analyzed using MS-Fit provided by UCSF (http://prospector.ucsf.edu/ucsfhtml3.2/msfit.htm).

Immunoblotting and Immunoprecipitation. Purified mitochondria were lysed and sonicated in RIPA buffer, then centrifuged at 16,000 rpm for 10 minutes. Protein concentration was determined using a BCA Protein Assay Reagent Kit (Pierce Biotechnology, Rockford, IL). The samples were separated by sodium dodecyl sulfate (SDS)-PAGE and electrotransferred onto a polyvinylidene fluoride membrane (Immobilon; Millipore, Japan), then blocked with BlockAce (Snow Brand, To-

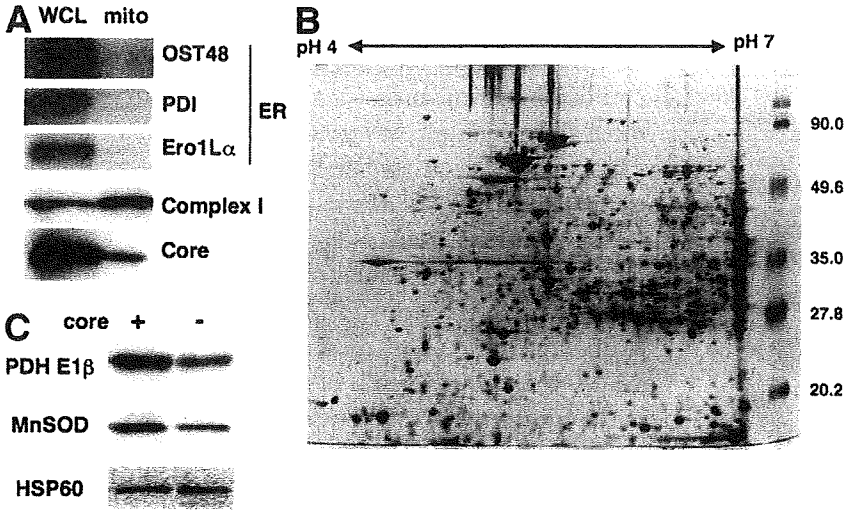

Fig. 1. 2D-PAGE of mitochondria purified from core-expressing cells. (A) Whole-cell lysates (WCL) and purified mitochondria (mito) derived from core-expressing cells were subjected to SDS-PAGE and immunoblotted with anti-core, anti-subunit of complex I (mitochondrial protein), or anti-OST48, PDI, Ero1La (ER proteins) antibodies. (B) Purified mitochondria of core-expressing cells were subjected to 2D-PAGE and the gel was stained with silver. The numbers shown on the right are molecular weights. (C) Purified mitochondria of core-expressing and control cells were subjected to SDS-PAGE and blotted with an anti-E1β subunit of PDH (PDH E1β), anti-MnSOD, or anti-HSP60 antibody.

kyo, Japan). The membrane was subsequently incubated with specific primary antibodies followed by horseradish peroxidase-conjugated secondary antibodies and visualized using SuperSignal West Pico Chemiluminescent Substrate (Pierce). Antibodies against the core protein (Anogen, Mississauga, Canada), manganese superoxide dismutase (MnSOD) (BD Biosciences, San Jose, CA), prohibitin (Neomarkers, Fremont, CA), oligosaccharyltransferase-48 (OST48), heat shock protein (HSP) 60 (Santa-Cruz Biotechnology, Santa Cruz, CA), pyruvate dehydrogenase (PDH), ubiquinol-cytochrome c oxidoreductase, COX (Molecular Probes, Eugene, OR), protein disulfide isomerase (PDI), ER protein endoplasmic oxidoreduction-1 (Ero1)-Lα, and IκBα (Cell Signaling Technology, Danvers, MA), were used as primary antibodies. For immunoprecipitation experiments, cells were lysed in NET-N buffer (20 mM Tris-HCl [pH 8.0], 100 mM NaCl, 1 mM EDTA, 0.5% Nonidet P-40) and the lysates were incubated with anti-prohibitin overnight followed by the addition of protein Sepharose 4B (GE Healthcare), then washed with the same buffer five times. Immunoprecipitates were subjected to SDS-PAGE followed by immunoblotting with specific antibodies.

Determination of COX Activity. COX activity was determined with a MitoProfile Rapid Microplate Assay Kit (MitoSciences, Eugene, OR) using 10 μg of purified mitochondria. The assay was performed three times independently.

Statistical Analysis. Results are expressed as means $\pm$ SE. The significance of the difference in means was determined by Student's *t* test or Mann-Whitney's *U* test.

Results

Presence of HCV Core Protein in Purified Mitochondria. Increasing evidence suggests that the HCV core protein is localized to mitochondria as well as to ER and the nucleus. Therefore, we first investigated whether the core protein is expressed in the mitochondria of core-expressing (Hep39) cells used in this study. We used Nycodenz discontinuous gradients to extract mitochondria as described.[17] In the mitochondria derived from core-expressing HepG2 cells, the core protein was detected by immunoblotting, whereas ER resident proteins such as an ER-specific type I transmembrane protein OST48, ER-resident molecular chaperon PDI, and ER membrane-associated N-glycoprotein Ero1-Lα, were not (Fig. 1A). In this fraction, reduced nicotinamide adenine dinucleotide (NADH)-ubiquinone oxidoreductase, complex I of mitochondrial oxidative phosphorylation system, was more strongly expressed than that in the whole cell. These results indicate that the purified mitochondria fraction was free of ER, and that a portion of the core protein was localized to the mitochondria in core-expressing cells.

Proteomics Analysis of Mitochondria by 2D-PAGE. For proteomics analysis, purified mitochondrial proteins derived from core-expressing cells were subjected to 2D-PAGE followed by silver-staining of the gel. In this study we analyzed only acidic proteins using IPG strips covering pH 4 to pH 7 because the analysis of acidic proteins by 2D-PAGE is relatively easy. The mitochondrial fraction was also extracted from Hepswx, a control cell line resistant to G418 but does not express the core protein, then similarly subjected to 2D-PAGE and used for comparing the expression pattern. We repeated the above procedure (purification of mitochondria, 2D-PAGE, and silver-staining) five times, and confirmed a similar expression pattern in core-expressing cells. The representative gel image is shown in Fig. 1B. ImageMaster 2D Elite software detected about 1100 spots on the silver-stained acidic gel, i.e., at pH 4-7 and Mrs of 20-100 kDa. The number of

Table 1. Proteins of Differential Expression in Mitochondria of Core-Expressing Cells

Protein Name	Fold Change (Mean ± SD)
Increased	
Succinyl-CoA:ketoacid CoA transferase	10.43 ± 1.29
NADH-specific isocitrate dehydrogenase a subunit precursor	9.64 ± 4.66
Unknown	8.65 ± 2.40
GrpE-like protein co-chaperon	5.71 ± 0.49
Leucine aminopeptidase	4.26 ± 1.14
Pyruvate dehydrogenase E1 component b subunit	3.79 ± 1.34
CGO15alt2	3.18 ± 0.80
HSP70	3.11 ± 1.39
Prohibitin	2.60 ± 0.24
3-Hydroxyisobutyrate dehydrogenase	2.47 ± 0.77
HSPC108	2.46 ± 0.69
MnSOD	2.35 ± 0.65
Ubiquinol-cytochrome c oxidoreductase core I protein	2.00 ± 0.23
Decreased	
Aldehyde dehydrogenase 2	0.12 ± 0.02
Aldehyde dehydrogenase 5 precursor	0.25 ± 0.03
ATP synthase a subunit isoform 1	0.50 ± 0.09
Reference protein	
HSP60	1.02 ± 0.02

protein spots was smaller than those reported in a recent study investigating the human placental mitochondrial proteome.[15]

We then compared the intensity of the spots between core-expressing and control cells. Analysis of repeated experiments by Student's t test revealed 13 increased and three decreased spots in intensity in core-expressing cells. These spots were excised and digested with trypsin, then proteins were identified by mass spectrometry. The names of the identified proteins are listed in Table 1. Among them were proteins related to mitochondrial respiratory chain, protein chaperons, and lipid metabolism. Because antibodies to some of these proteins are commercially available, expression levels of the proteins were examined by immunoblotting. The expression levels of the PDH-E1β subunit and MnSOD, which were identified as increased proteins, were higher in core-expressing cells than in control cells (Fig. 1C), whereas that of HSP60, which was identified as having a similar expression, was unchanged.

Up-regulation of Prohibitin by the Core Protein. Among the identified proteins, we focused on prohibitin, an up-regulated protein in mitochondria of core-expressing cells (Fig. 2A). Prohibitin is a mitochondrial protein associated with cell proliferation.[20] It also works as a chaperon of mitochondrial proteins.[21,22] We confirmed an increased prohibitin expression level in core-expressing cells

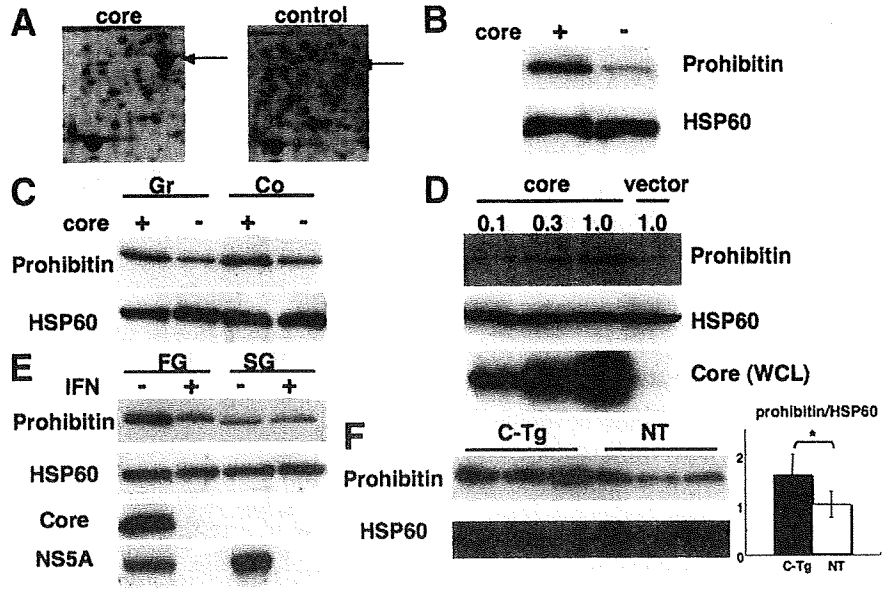

Fig. 2. Up-regulation of prohibitin in core-expressing cells. (A) Protein spot corresponding to prohibitin (arrow) in 2D-PAGE. (B) Purified mitochondria from core-expressing or control cells were subjected to SDS-PAGE and immunoblotted with anti-prohibitin or anti-HSP60 antibody. (C) Mitochondria were purified from growing (Gr) or confluent (Co) cells in 100-mm dishes and subjected to SDS-PAGE, then immunoblotted with an anti-prohibitin or anti-HSP60 antibody. (D) HepG2 cells in six-well plates were transfected with different amounts (μg) of core-expressing plasmid and mitochondrial proteins were analyzed by immunoblotting with anti-prohibitin or anti-HSP60 antibody. The expression levels of the core protein in whole-cell lysates (WCL) were also determined. (E) Cells harboring HCV replicon were untreated or treated with IFN and expression levels of prohibitin in mitochondria were determined. Expression of HCV core and NS5A proteins was also examined. FG, full-genomic replicon cells; SG, subgenomic replicon cells. (F) Expression levels of prohibitin in mitochondria were determined in liver tissues HCV core-gene transgenic and nontransgenic mice. Prohibitin/HSP60 expression levels were determined by densitometry. C-Tg, core-gene transgenic mouse; NT, nontransgenic littermate ($n = 3$) $^*P < 0.05$.

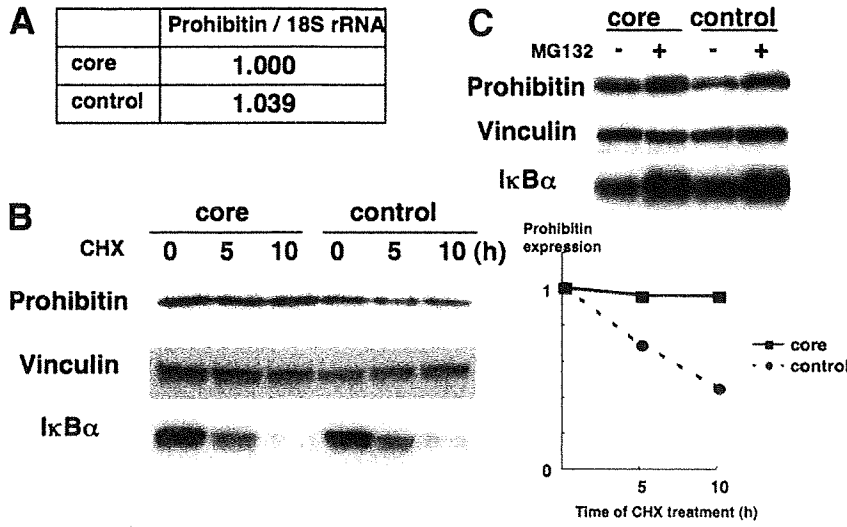

Fig. 3. Increased protein stability of prohibitin in core-expressing cells. (A) RNA was extracted from core-expressing and control cells, and the amount of specific mRNA was determined by real-time PCR with specific primers/probe against prohibitin. The amount of prohibitin mRNA was standardized by that of 18S ribosomal RNA (18S rRNA). (B) Cells were incubated with 100 ng/mL cycloheximide and harvested at the timepoints indicated above the lanes (numbers are hours of cycloheximide treatment). Whole-cell lysates were subjected to SDS-PAGE and immunoblotted with anti-prohibitin, anti-IκBα, or anti-vinculin (as an internal standard) antibody. The intensity of each band was measured by densitometry, and expression levels (prohibitin/vinculin) are shown in the right panel. (C) Cells were harvested after incubation with 20 μM MG132 for 8 hours and subjected to immunoblotting with anti-prohibitin, anti-IκBα, or anti-vinculin antibody.

by immunoblotting (Fig. 2B). Because prohibitin is associated with cell proliferation, it is possible that prohibitin expression changed according to the cell proliferative status. As shown in Fig. 2C, core-expressing cells had high prohibitin expression levels in the cells in both confluent growth and growing statuses compared with control cells. We also determined the expression levels in cells synchronized with aphidicolin followed by l-mimosine treatment and found an increased expression level in core-expressing cells (data not shown). To exclude the possibility that the increased prohibitin expression level is due to the expansion of limited cell clones, not specific to the core protein expression, we examined prohibitin expression in cells transiently expressing the core protein and found that prohibitin expression level increased dose-dependently in core-expressing cells (Fig. 2D). We also examined the prohibitin expression levels in Huh7 cells harboring full- or subgenomic HCV replicon. For this purpose, we used interferon (IFN)-treated replicon cells (cured cells) as a control. Core and nonstructural (NS)5A proteins were not detected after treatment of full-genomic replicon cells with IFN, suggesting a successful elimination of replicon. Prohibitin expression levels in cells with full-genomic replicon were increased compared with those in IFN-treated cured cells, whereas levels of prohibitin expression were low in subgenomic replicon cells regardless of IFN-treatment (Fig. 2E). In addition, prohibitin expression levels were also increased in livers of 3-month-old transgenic mice expressing the core protein compared with those in nontransgenic littermates (Fig. 2F).

We next sought to determine the mechanism of the increased steady-state level of prohibitin in core-expressing cells. To determine prohibitin messenger RNA (mRNA) expression, we performed a real-time polymerase chain reaction (PCR) using specific primers/probe. No difference in prohibitin mRNA was observed between core-expressing and control cells (Fig. 3A). We next determined the stability of prohibitin in these cells. By treating the cells with cycloheximide, the expression levels of prohibitin gradually decreased in control cells (Fig. 3B). On the other hand, in core-expressing cells prohibitin was hardly degraded by cycloheximide treatment for 10 hours, whereas IκBα was equally degraded in both cells. This result suggests that prohibitin was stabilized in the presence of the core protein. Because prohibitin has been shown to be degraded by proteasome,[23] we examined expression levels of prohibitin in the presence of proteasome inhibitor MG132. By treatment with MG132, prohibitin expression was increased to the similar level in core-expressing and control cells. These results suggest that the core protein may inhibit proteasomal degradation of prohibitin by some mechanism, including the prevention of degradation by interaction with the core protein. Then, core-expressing cells were lysed and subjected to immunoprecipitation with an anti-prohibitin antibody. As shown in Fig. 4, the core protein was coimmunoprecipitated with an anti-prohibitin antibody. To exclude a nonspecific interaction with the antibody or Sepharose beads, cells expressing a small amount of prohibitin by transfection with small interfering RNA (siRNA) against prohibitin were also examined. In these cells the amount of the coimmunoprecipitated core protein decreased. In addition, the core protein was not coimmunoprecipitated by control immunoglobulin G (IgG), indicating a specific interaction of prohibitin with the core protein. These results suggest that prohibitin expression increased in core-expressing cells owing to the increased stability presumably by interaction with the core protein.

Impaired Chaperon Function of Prohibitin in Core-Expressing Cells. We next examined the effect of

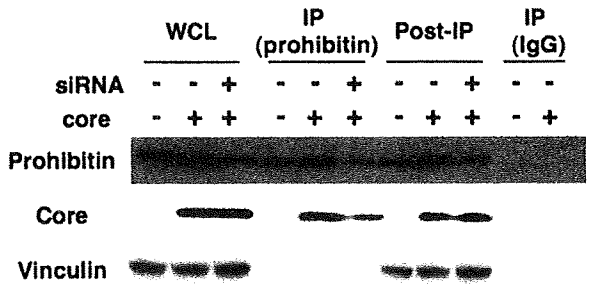

Fig. 4. Interaction of the core protein with prohibitin. Core-expressing and control cells were transfected with or without siRNA against the prohibitin gene, then harvested and lysed in NET-N buffer 3 days after transfection. Whole-cell lysates (WCL) were immunoprecipitated (IP) with an anti-prohibitin antibody or control IgG and immunoblotted with anti-prohibitin or anti-core antibody. Supernatants after the immunoprecipitation were harvested and similarly immunoblotted (Post-IP).

the interaction of prohibitin with the core protein on the function of prohibitin. Prohibitin works as a chaperon of mitochondrial proteins. Nijtmans et al.[21] demonstrated that prohibitin exerts a chaperon function particularly for the stabilization of mitochondrial DNA-encoded proteins. COX is a mitochondrial respiratory complex IV formed by 14 subunits, 10 of which are encoded by nuclear DNA and the rest by mitochondrial DNA.[24] We examined the interaction of prohibitin with subunit II of COX encoded by mitochondrial DNA. As shown in Fig. 5A, the level of COX II coimmunoprecipitated with an anti-prohibitin antibody was decreased in core-expressing cells, although the amount of immunoprecipitated prohibitin was higher than that in control cells. On the other hand, the subunit IV of COX encoded by nuclear DNA was similarly coimmunoprecipitated between core-expressing and control cells. When prohibitin expression was decreased by siRNA transfection, coimmunoprecipitation of COX subunits was similarly decreased with the amount of immunoprecipitation of prohibitin itself being low. We next determined expression levels of COX subunits in the mitochondria in these cells. Expression levels of mitochondrial DNA-encoded subunits I and II in core-expressing cells were decreased, whereas the levels of nuclear DNA-encoded subunits IV and VIb were similar to those in control cells. When transfected with prohibitin-siRNA, expression levels of all of the COX subunits examined were decreased in both core-expressing and control cells, suggesting that protein levels of these subunits are dependent on prohibitin (Fig. 5B, see Supporting Fig. 1 for densitometry). Similar data were observed when blots for COX II and IV were developed together in the same membrane (Supporting Fig. 2). We also determined COX activity in these cells and found that core-expressing cells had a significantly decreased COX activity (about 70% of that in control cells, Fig. 5C). These results suggest that interaction of prohibitin with the core protein is associated with an impaired function of prohibitin as a mitochondrial chaperon, which may trigger disordered assembly and function of mitochondrial respiratory complexes.

Discussion

In the present study we analyzed expression levels of mitochondrial proteins in HepG2 cells expressing the HCV core protein and identified a set of proteins with different expressions. Some of those proteins were related to the mitochondrial respiratory chain (Table 1). Because the core protein was shown to be associated with the induction of oxidative stress,[7-9] the core protein may modulate the expression and function of proteins forming mitochondrial respiratory complexes, which naturally

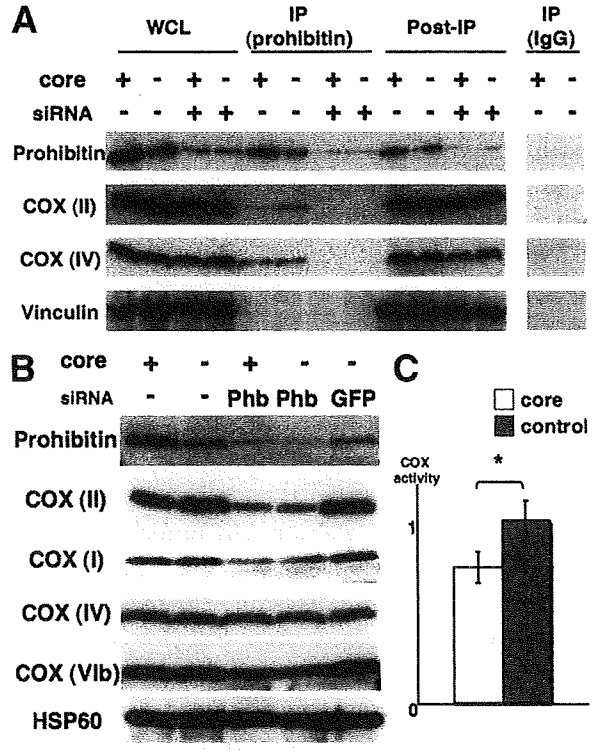

Fig. 5. Effects of core-prohibitin interaction on interaction/expression of COX subunit proteins and COX activity. (A) Whole-cell lysates (WCL) of core-expressing and control cells were subjected to immunoprecipitation with an anti-prohibitin antibody or control IgG, and the interaction of prohibitin with COX subunits was determined by immunoblotting of immunoprecipitated proteins (IP). Supernatants after the immunoprecipitation were harvested and similarly immunoblotted (Post-IP). (B) Cells were transfected with or without siRNA against the prohibitin (Phb) or GFP gene and harvested 3 days after transfection for purification of mitochondria. Purified mitochondria were subjected to SDS-PAGE and immunoblotted with several anti-COX subunits antibodies. The expression levels of HSP60 were also examined as an internal control. (C) COX activity was determined by measuring cytochrome c oxidation. The activity was normalized by taking the average rate of control cells as 1. Data shown are means ± SE (n = 5). *$P < 0.05$.

leads to ROS accumulation. In addition, MnSOD, which plays a key role in protecting cells from oxidative damage, was up-regulated in core-expressing cells, reflecting ROS increase in the cells. Several protein chaperons such as HSP70 and GrpE-like protein co-chaperon were also identified as up-regulated proteins. Because these proteins are known to be important in the mitochondrial protein-import mechanisms, the modulated expression of these proteins may be associated with the different expressions of the identified mitochondrial proteins.

Prohibitin, a mitochondrial protein chaperon, was identified as an up-regulated protein in core-expressing cells. Prohibitin is a ubiquitously expressed and highly conserved protein that was originally determined to play a predominant role in inhibiting cell-cycle progression and cellular proliferation by attenuating DNA synthesis.[20,25] Prohibitin is present in the nucleus and interacts with transcription factors that are important in cell cycle progression. In core-expressing cells used in this study, prohibitin was also detected in the nucleus and its expression level was also higher than that in control Hepswx cells or HepG2 cells (data not shown). The growth rate of core-expressing cells, however, was similar to that of control cells (data not shown). The physiological significance of the high expression level of prohibitin in the nucleus remains to be determined, but it may be related to enhanced apoptosis by Fas ligand, as shown by Ruggieri et al.,[16] because prohibitin interacts with E2F, Rb, and p53 and modulates the transcription activity of these factors and induces apoptosis.[26,27]

Mitochondrial prohibitin acts as a protein chaperon by stabilizing newly synthesized mitochondrial translation products through direct interaction.[21] We examined the interaction between prohibitin and mitochondrially encoded subunit II of COX and found a suppressed interaction between these proteins in core-expressing cells. In addition, there are several studies that showed the association of prohibitin with the assembly of mitochondrial respiratory complex I as well as complex IV (COX).[21,28] Complex I also consists of both nuclear- and mitochondrial-DNA-encoded subunits; therefore, it is probable that the assembly and function of complex I are impaired by the core protein. We attempted to examine the interaction of prohibitin with the mitochondrial DNA-encoded subunit of complex I, but commercially available antibodies against this subunit could not detect the protein itself by immunoblotting (data not shown). With respect to the complex I function, we found a decreased complex I activity in core-expressing cells (H. Miyoshi et al., manuscript in preparation). Other groups have also shown that complex I activity is decreased in the liver of transgenic mice harboring HCV core and envelope genes[9] as well as in cultured cells.[29] From these findings, the interaction between prohibitin and the core protein may impair the function of complex I as well as complex IV, leading to an increase in ROS production. In fact, the suppression of the prohibitin function is shown to result in an increased production of ROS,[30] a phenomenon observed in core-expressing cells used in this study (Miyoshi et al., in prep.) as well as in the liver of core-gene transgenic mice.[7,8] Interestingly, Berger and Yaffe[31] showed that loss of function of prohibitin leads to an altered mitochondrial morphology, that is, the loss of the normal reticular morphology and organized mitochondrial distribution. In hepatocytes from the core-gene transgenic mice, we observed a change in morphology of mitochondria, a disappearance of the double structure of mitochondrial membranes.[2] These changes in mitochondrial morphology are somewhat different, but the dysfunction of prohibitin may be responsible for the morphological abnormality of mitochondria observed in the core-gene transgenic mice.

We concluded that prohibitin overexpression is due to increased stability induced by the interaction with the core protein. In this study we showed that prohibitin might be degraded by proteasome, although we could not detect ubiquitinated forms of prohibitin. If the degradation is mediated by ubiquitin as reported,[23] it is possible that the interaction with the core protein interferes with ubiquitin-binding and protects prohibitin from degradation by proteasome. Some posttranslational protein modifications such as phosphorylation are other possible factors for the stabilization, because prohibitin can be serine-phosphorylated[32]; however, in our examination no serine/threonine/tyrosine phosphorylation of prohibitin was detected in core-expressing cells (data not shown). Thus far, there are no studies showing that prohibitin stabilization leads to a suppressed function as a mitochondrial chaperon. Therefore, this finding is novel and noteworthy because the prohibitin expression level has been considered to be proportional to the chaperon function. Prohibitin is highly expressed in several human tumors.[33,34] In addition, a 2D-PAGE of the hepatoma cell line HCC-M identified prohibitin as a positively regulated protein.[35] In these studies, the mechanism of prohibitin overexpression was not elucidated, but considering that prohibitin is associated with the inhibition of cell proliferation, the function of prohibitin is suppressed by stabilization by some molecules in the tumor, similar to the mechanism we suggest in the current study.

In addition to HepG2 cells constitutively expressing the core protein, increased prohibitin expression levels were also found in livers of core-gene transgenic mice.

The difference in expression levels between the transgenic mice and nontransgenic littermates, however, was a little bit smaller than that in the studies of HepG2 cells. This may be due to the low expression level of the core protein in the transgenic mice compared with that in core-expressing HepG2 cells because the expression level of prohibitin was proportionally increased to that of the core protein as shown in this study (Fig. 2D). Otherwise, there might be some *in vivo* mechanism for suppressing prohibitin expression in mice.

In this study, COX subunit IV as well as II were found to interact with prohibitin (Fig. 5A). Although there are no studies demonstrating that prohibitin also works as chaperon for nuclear DNA-encoded mitochondrial proteins as far as we investigated, knockdown of prohibitin expression by siRNA led to decreases in expression levels of both nuclear (COX IV, VIb) and mitochondrial (COX I, II) DNA-encoded subunits in mitochondria (Fig. 5B and Supporting Figs. 1 and 2). We showed that COX IV interacts with prohibitin (Fig. 4), suggesting that prohibitin also works for stable expression of nuclear DNA-encoded COX IV. Degrees of decrease in COX IV and VIb expression, however, were smaller than those in I and II. Prohibitin might contribute to stabilization of COX IV and VIb by mechanism(s) other than chaperon function. Steglich et al.[36] showed that prohibitin regulates protein degradation by the m-AAA protease in mitochondria. Recently, Da Cruz et al.[37] showed that SLP-2, a member of the stomatin gene family, interacts with prohibitin and regulates the expression of mitochondrial proteins such as COX IV and ND6 of complex I encoded by nuclear DNA by AAA proteases. In view of these findings, COX IV and VIb expression in mitochondria is dependent on prohibitin but other factors may also be involved in the attainment of stable expression of these subunits. The expression levels of COX II and IV in the whole-cell lysates were not so drastic among cell samples (Fig. 5A) compared to those in the mitochondria (Fig. 5B). The reason is not clear, but it is possible that redundant proteins such as improperly folded proteins by lack of chaperons were included in the whole-cell lysates.

In summary, we analyzed mitochondrial proteins in core-expressing HepG2 cells by proteomics analysis and identified prohibitin as an up-regulated protein. The dysfunction of prohibitin induced by the core protein may lead to ROS overproduction in the mitochondrion, which plays a key role in the pathogenesis of chronic hepatitis C. The restoration of prohibitin function might be a therapeutic option for correcting the dysregulated assembly and dysfunction of mitochondrial respiratory chain complexes.

Acknowledgment: We thank S. Shinzawa, M. Yahata, and S. Yoshizaki for technical assistance.

References

1. Suzuki R, Suzuki T, Ishii K, Matsuura Y, Miyamura T. Processing and functions of Hepatitis C virus proteins. Intervirology 1999;42:145-152.
2. Moriya K, Fujie H, Shintani Y, Yotsuyanagi H, Tsutsumi T, Ishibashi K, et al. The core protein of hepatitis C virus induces hepatocellular carcinoma in transgenic mice. Nat Med 1998;4:1065-1067.
3. Naas T, Ghorbani M, Alvarez-Maya I, Lapner M, Kothary R, De Repentigny Y, et al. Characterization of liver histopathology in a transgenic mouse model expressing genotype 1a hepatitis C virus core and envelope proteins 1 and 2. J Gen Virol 2005;86:2185-2196.
4. Machida K, Cheng KT, Lai CK, Jeng KS, Sung VM, Lai MM. Hepatitis C virus triggers mitochondrial permeability transition with production of reactive oxygen species, leading to DNA damage and STAT3 activation. J Virol 2006;80:7199-7207.
5. Suzuki R, Sakamoto S, Tsutsumi T, Rikimaru A, Tanaka K, Shimoike T, et al. Molecular determinants for subcellular localization of hepatitis C virus core protein. J Virol 2005;79:1271-1281.
6. Schwer B, Ren S, Pietschmann T, Kartenbeck J, Kaehlcke K, Bartenschlager R, et al. Targeting of hepatitis C virus core protein to mitochondria through a novel C-terminal localization motif. J Virol 2004;78:7958-7968.
7. Moriya K, Nakagawa K, Santa T, Shintani Y, Fujie H, Miyoshi H, et al. Oxidative stress in the absence of inflammation in a mouse model for hepatitis C virus-associated hepatocarcinogenesis. Cancer Res 2001;61:4365-4370.
8. Okuda M, Li K, Beard MR, Showalter LA, Scholle F, Lemon SM, et al. Mitochondrial injury, oxidative stress, and antioxidant gene expression are induced by hepatitis C virus core protein. Gastroenterology 2002;122:366-375.
9. Korenaga M, Wang T, Li Y, Showalter LA, Chan T, Sun J, et al. Hepatitis C virus core protein inhibits mitochondrial electron transport and increases reactive oxygen species (ROS) production. J Biol Chem 2005;280:37481-37488.
10. Diamond DL, Jacobs JM, Paeper B, Proll SC, Gritsenko MA, Carithers RL Jr, et al. Proteomic profiling of human liver biopsies: hepatitis C virus-induced fibrosis and mitochondrial dysfunction. HEPATOLOGY 2007;46:649-657.
11. Moriya K, Yotsuyanagi H, Shintani Y, Fujie H, Ishibashi K, Matsuura Y, et al. Hepatitis C virus core protein induces hepatic steatosis in transgenic mice. J Gen Virol 1997;78(Pt 7):1527-1531.
12. Moriya K, Todoroki T, Tsutsumi T, Fujie H, Shintani Y, Miyoshi H, et al. Increase in the concentration of carbon 18 monounsaturated fatty acids in the liver with hepatitis C: analysis in transgenic mice and humans. Biochem Biophys Res Commun 2001;281:1207-1212.
13. Fujie H, Yotsuyanagi H, Moriya K, Shintani Y, Tsutsumi T, Takayama T, et al. Steatosis and intrahepatic hepatitis C virus in chronic hepatitis. J Med Virol 1999;59:141-145.
14. Cho WC. Contribution of oncoproteomics to cancer biomarker discovery. Mol Cancer 2007;6:25.
15. Lescuyer P, Strub JM, Luche S, Diemer H, Martinez P, Van Dorsselaer A, et al. Progress in the definition of a reference human mitochondrial proteome. Proteomics 2003;3:157-167.
16. Ruggieri A, Harada T, Matsuura Y, Miyamura T. Sensitization to Fas-mediated apoptosis by hepatitis C virus core protein. Virology 1997;229:68-76.
17. Okado-Matsumoto A, Fridovich I. Subcellular distribution of superoxide dismutases (SOD) in rat liver: Cu,Zn-SOD in mitochondria. J Biol Chem 2001;276:38388-38393.
18. Murakami K, Ishii K, Ishihara Y, Yoshizaki S, Tanaka K, Gotoh Y, et al. Production of infectious hepatitis C virus particles in three-dimensional cultures of the cell line carrying the genome-length dicistronic viral RNA of genotype 1b. Virology 2006;351:381-392.

19. Shevchenko A, Wilm M, Vorm O, Mann M. Mass spectrometric sequencing of proteins silver-stained polyacrylamide gels. Anal Chem 1996;68: 850-858.
20. Mishra S, Murphy LC, Murphy LJ. The prohibitins: emerging roles in diverse functions. J Cell Mol Med 2006;10:353-363.
21. Nijtmans LG, de Jong L, Artal Sanz M, Coates PJ, Berden JA, Back JW, et al. Prohibitins act as a membrane-bound chaperone for the stabilization of mitochondrial proteins. EMBO J 2000;19:2444-2451.
22. Back JW, Sanz MA, De Jong L, De Koning LJ, Nijtmans LG, De Koster CG, et al. A structure for the yeast prohibitin complex: structure prediction and evidence from chemical crosslinking and mass spectrometry. Protein Sci 2002;11:2471-2478.
23. Thompson WE, Ramalho-Santos J, Sutovsky P. Ubiquitination of prohibitin in mammalian sperm mitochondria: possible roles in the regulation of mitochondrial inheritance and sperm quality control. Biol Reprod 2003; 69:254-260.
24. Fontanesi F, Soto IC, Horn D, Barrientos A. Assembly of mitochondrial cytochrome c-oxidase, a complicated and highly regulated cellular process. Am J Physiol Cell Physiol 2006;291:C1129-C1147.
25. Mishra S, Murphy LC, Nyomba BL, Murphy LJ. Prohibitin: a potential target for new therapeutics. Trends Mol Med 2005;11:192-197.
26. Fusaro G, Dasgupta P, Rastogi S, Joshi B, Chellappan S. Prohibitin induces the transcriptional activity of p53 and is exported from the nucleus upon apoptotic signaling. J Biol Chem 2003;278:47853-47861.
27. Joshi B, Ko D, Ordonez-Ercan D, Chellappan SP. A putative coiled-coil domain of prohibitin is sufficient to repress E2F1-mediated transcription and induce apoptosis. Biochem Biophys Res Commun 2003;312:459-466.
28. Bourges I, Ramus C, Mousson de Camaret B, Beugnot R, Remacle C, Cardol P, et al. Structural organization of mitochondrial human complex I: role of the ND4 and ND5 mitochondria-encoded subunits and interaction with prohibitin. Biochem J 2004;383:491-499.
29. Piccoli C, Scrima R, Quarato G, D'Aprile A, Ripoli M, Lecce L, et al. Hepatitis C virus protein expression causes calcium-mediated mitochondrial bioenergetic dysfunction and nitro-oxidative stress. HEPATOLOGY 2007;46:58-65.
30. Theiss AL, Idell RD, Srinivasan S, Klapproth JM, Jones DP, Merlin D, et al. Prohibitin protects against oxidative stress in intestinal epithelial cells. FASEB J 2007;21:197-206.
31. Berger KH, Yaffe MP. Prohibitin family members interact genetically with mitochondrial inheritance components in Saccharomyces cerevisiae. Mol Cell Biol 1998;18:4043-4052.
32. Ross JA, Nagy ZS, Kirken RA. The PHB1/2 phosphocomplex is required for mitochondrial homeostasis and survival of human T cells. J Biol Chem 2008;283:4699-4713.
33. Coates PJ, Nenutil R, McGregor A, Picksley SM, Crouch DH, Hall PA, et al. Mammalian prohibitin proteins respond to mitochondrial stress and decrease during cellular senescence. Exp Cell Res 2001;265:262-273.
34. Asamoto M, Cohen SM. Prohibitin gene is overexpressed but not mutated in rat bladder carcinomas and cell lines. Cancer Lett 1994;83:201-207.
35. Seow TK, Ong SE, Liang RC, Ren EC, Chan L, Ou K, et al. Two-dimensional electrophoresis map of the human hepatocellular carcinoma cell line, HCC-M, and identification of the separated proteins by mass spectrometry. Electrophoresis 2000;21:1787-1813.
36. Steglich G, Neupert W, Langer T. Prohibitins regulate membrane protein degradation by the m-AAA protease in mitochondria. Mol Cell Biol 1999; 19:3435-3442.
37. Da Cruz S, Parone PA, Gonzalo P, Bienvenut WV, Tondera D, Jourdain A, et al. SLP-2 interacts with prohibitins in the mitochondrial inner membrane and contributes to their stability. Biochim Biophys Acta 2008;1783: 904-911.

[a]*Avon Orthopaedic Centre, Bristol, UK*
[b]*Department of Microbiology, Southmead Hospital, Bristol, UK*
E-mail address: alannapentlow@doctors.org.uk

Available online 28 August 2009

* Corresponding author. Address: Department of Microbiology, Southmead Hospital, Southmead Road, Bristol BS10 5NB, UK. Tel.: +44 797 618 8454; fax: +44 117 959 5901.

doi:10.1016/j.jhin.2009.06.014

Evaluation of the efficacy of a low temperature steam and formaldehyde steriliser by using biological indicators

Madam,

Medical instruments, such as rigid and flexible operative endoscopes, including accessories, must be sterilised using properly validated processes.[1] Laparoscopic, urological and arthroscopic telescopes and their accessories are now largely heat tolerant and may be autoclaved, but nevertheless some are heat labile, as are all flexible fibreoptic or video endscopes. These are best sterilised using ethylene oxide (EO), gas plasma or low temperature steam and formaldehyde (LTSF).[1] LTSF sterilisers are used in European countries, and their usefulness and safety for sterilisation of heat-labile materials has been reported.[2–4] In this study, we evaluated the efficacy of an LTSF steriliser, Matachana 130LF (Matachana, Barcelona, Spain) by using biological indicators (BIs).

The LTSF steriliser Matachana 130LF, which fulfils all the requirements of the forthcoming European Norm for LTSF sterilisers (EN 14180, EN 61326-1, EN 60204-1, EN 61010-1 and EN 61010-2-042), was used. The sterilisation cycle consists of six phases: pre-vacuum, pre-pulses of steam, formaldehyde feed, sterilisation, washing pulses, and air pulses. Three BIs including *Geobacillus stearothermophilus* ATCC 7953 were used to assess sterilisation: a filter paper containing 2.3×10^6 spores (Statens Serum Institute, Copenhagen, Denmark) (SSI BI), a filter paper containing 1.7×10^6 spores (SGM, Bozeman, MT) (SGM BI) and a filter paper containing 1.9×10^5 spores (Simicon, Munich, Germany). A BI was placed into a process challenge device (PCD) which was made by Udono Co., Inc. (Tokyo, Japan) based on a standard of EN 14180 and was packed in a sterilisation bag (Sengewald, Rohrdorf, Germany) attached to the chemical indicators for LTSF before sterilisation. For the sterilisation temperature of 60 °C, the times of sterilisation processes were 5, 10, 15, 20, and 30 min. After the sterilisation process was completed, the filter paper was removed from the PCD and placed in a test tube with 10 mL tryptone soya broth (CM0129, Oxoid, Basingstoke, UK). The filter paper was cultured at 56 °C for 7 days. Positive results were inferred when turbidity was seen with the naked eye. Gram-positive bacilli were confirmed by Gram stain and were identified by using the Vitek 1 system (Sysmex-bioMérieux, Tokyo, Japan). An unsterilised BI was used as the positive control for each experiment. All experiments were repeated four times.

A total of 56 BIs were cultured and results are shown in Table I. Although the cultures of the SSI BIs following 5, 10, and 15 min sterilisation cycles were positive, the culture of the remaining BIs yielded no growth. Bacterial growth was present in all the positive control cultures and it confirmed that the positive sample was *G. stearothermophilus*. The number of spores contained in the SSI BI (2.3×10^6 spores) is 1.4 and 12 times that of the SGM BI (1.7×10^6 spores) and the Simicon BI (1.9×10^5 spores), respectively. Using *G. stearothermophilus* ATCC 7953 at more than 10^5 spores as a BI for LTSF is recommended with the standard (ISO 11138-5 and EN 866-5). Hence, when the sterilisation process used a programme temperature of 60 °C it could be suggested that the sterilisation process would need to be longer than 20 min. Moreover, no growth was seen in cultures for reference strains, clinical and environmental isolates,

Table I Sterilisation time at 60 °C and growth of biological indicators after low temperature steam and formaldehyde sterilisation

Sterilisation (min)	Biological indicators (spores)		
	SSI[a] (2.3×10^6)	SGM (1.7×10^6)	Simicon (1.9×10^5)
5	+ (3)	–	–
10	+ (1)	–	–
15	+ (1)	–	–
20	–	–	–
30	–	–	NT

+, culture positive (the number of positive samples); –, culture negative; NT, not tested.
[a] Statens Serum Institute.

such as *Escherichia coli* ATCC 25922, *Pseudomonas aeruginosa* ATCC 27853, *Staphylococcus aureus* ATCC 25923, *Streptococcus pneumoniae* ATCC 6305, *Haemophilus influenzae* ATCC 35056, meticillin-resistant *S. aureus* (clinical isolate), extended spectrum β-lactamase-producing *E. coli* (clinical isolate), metallo β-lactamase-producing *P. aeruginosa* (clinical isolate), multidrug-resistant *P. aeruginosa* (clinical isolate), *Pseudomonas putida* (environmental isolate), *Acinetobacter* spp. (environmental isolate), Candida albicans (environmental isolate).

Some medical equipment, such as endoscopes, may be used more than once a day. This study demonstrated that sterilisation temperature of less than 60 °C requires a cycle time of more than 20 min. Although an EO gas steriliser requires at least 24 h, the LTSF steriliser requires only 3.5 h.[4] Additionally, the LTSF steriliser has been reported as an adequate and reliable method for flexible endoscopes.[4,5] Furthermore, the formaldehyde residues after LTSF sterilisation were all below the value as indicated by the EN 14180 in the present study (data not shown). In conclusion, the benefits of LTSF sterilisation are efficacy, short cycle time, and safety.

Conflict of interest statement
None declared.

Funding sources
None.

References

1. Ayliffe G. Decontamination of minimally invasive surgical endoscopes and accessories. *J Hosp Infect* 2000;45: 263–277.
2. Gibson GL. Processing heat-sensitive instruments and materials by low-temperature steam and formaldehyde. *J Hosp Infect* 1980;1:95–101.
3. Robertshaw RG. Low temperature steam and formaldehyde sterilization. *J Hosp Infect* 1983;4:305–314.
4. Kanemitsu K, Kunishima H, Imasaka T, *et al*. Evaluation of a low-temperature steam and formaldehyde sterilizer. *J Hosp Infect* 2003;55:47–52.
5. Adler S, Scherrer M, Daschner FD. Costs of low-temperature plasma sterilization compared with other sterilization methods. *J Hosp Infect* 1998;40:125–134.

R. Saito[a,*]
Y. Uetera[b]
Y. Saito[b]
N. Okamura[c]
K. Moriya[a]
K. Koike[a]

[a]*Department of Infection Control and Prevention, University of Tokyo Hospital, Tokyo, Japan*
[b]*Department of Hospital Environment, Surgical Center, University of Tokyo Hospital, Tokyo, Japan*
[c]*Department of Microbiology and Immunology, Graduate School of Health Sciences, Tokyo Medical and Dental University, Tokyo, Japan*
E-mail address: saito-lab@umin.ac.jp

Available online 22 August 2009

* Corresponding author. Address: Department of Infection Control and Prevention, University of Tokyo Hospital, 7-3-1 Hongo, Bunkyo-ku, Tokyo 113-8655, Japan. Tel.: +81 3 3815 5411x35028; fax: +81 3 5689 0495.

doi:10.1016/j.jhin.2009.06.018

Combined effect of copper and silver against *Pseudomonas aeruginosa*

Madam,

Infection from *Pseudomonas aeruginosa* is an increasing cause for concern in the healthcare environment and it is associated with chronic lung infections, particularly in patients with cystic fibrosis. The Health Protection Agency has reported a 20% increase in cases of *P. aeruginosa* nosocomial infections since 2003. *P. aeruginosa* exhibits multiple drug resistance and it is feared that a total drug resistance will eventually emerge.[1]

Copper and silver both have an antimicrobial effect against a range of pathogens, with a ≥ 2.5 $\log_{10}$ reduction observed against *Clostridium difficile* after 3 h exposure to copper surfaces and a 3 $\log_{10}$ cfu/mL increased reduction in meticillin-resistant *Staphylococcus aureus* from silver-impregnated wound dressings compared to controls.[2,3]

There is limited published research on the antimicrobial synergy between copper and silver; therefore, an investigation was conducted to assess their combined antimicrobial effect against *P. aeruginosa*.

The micro-organism tested was *Pseudomonas aeruginosa* ATCC 10145, grown in nutrient broth (CM0001) and cultured on nutrient agar (CM0003, Oxoid Ltd, Basingstoke, UK). Minimum inhibitory

nature genetics

Genome-wide association of *IL28B* with response to pegylated interferon-α and ribavirin therapy for chronic hepatitis C

Yasuhito Tanaka[1,18], Nao Nishida[2,18], Masaya Sugiyama[1], Masayuki Kurosaki[3], Kentaro Matsuura[1], Naoya Sakamoto[4], Mina Nakagawa[4], Masaaki Korenaga[5], Keisuke Hino[5], Shuhei Hige[6], Yoshito Ito[7], Eiji Mita[8], Eiji Tanaka[9], Satoshi Mochida[10], Yoshikazu Murawaki[11], Masao Honda[12], Akito Sakai[12], Yoichi Hiasa[13], Shuhei Nishiguchi[14], Asako Koike[15], Isao Sakaida[16], Masatoshi Imamura[17], Kiyoaki Ito[17], Koji Yano[17], Naohiko Masaki[17], Fuminaka Sugauchi[1], Namiki Izumi[3], Katsushi Tokunaga[2] & Masashi Mizokami[1,17]

The recommended treatment for patients with chronic hepatitis C, pegylated interferon-α (PEG-IFN-α) plus ribavirin (RBV), does not provide sustained virologic response (SVR) in all patients. We report a genome-wide association study (GWAS) to null virological response (NVR) in the treatment of patients with hepatitis C virus (HCV) genotype 1 within a Japanese population. We found two SNPs near the gene *IL28B* on chromosome 19 to be strongly associated with NVR (rs12980275, $P = 1.93 \times 10^{-13}$, and rs8099917, 3.11×10^{-15}). We replicated these associations in an independent cohort (combined P values, 2.84×10^{-27} (OR = 17.7; 95% CI = 10.0–31.3) and 2.68×10^{-32} (OR = 27.1; 95% CI = 14.6–50.3), respectively). Compared to NVR, these SNPs were also associated with SVR (rs12980275, $P = 3.99 \times 10^{-24}$, and rs8099917, $P = 1.11 \times 10^{-27}$). In further fine mapping of the region, seven SNPs (rs8105790, rs11881222, rs8103142, rs28416813, rs4803219, rs8099917 and rs7248668) located in the *IL28B* region showed the most significant associations ($P = 5.52 \times 10^{-28}$–2.68×10^{-32}; OR = 22.3–27.1). Real-time quantitative PCR assays in peripheral blood mononuclear cells showed lower *IL28B* expression levels in individuals carrying the minor alleles ($P = 0.015$).

Hepatitis C is a global health problem that affects a significant proportion of the world's population. The World Health Organization estimated that in 1999, there were 170 million HCV carriers worldwide, with 3–4 million new cases appearing each year. HCV infection affects more than 4 million people in the United States, where it represents the leading cause of cirrhosis and hepatocellular carcinoma as well as the leading cause of liver transplantation[1].The American Gastroenterological Association estimated that drugs are the largest direct costs of hepatitis C[1].

The most effective current standard of care in patients with chronic hepatitis C, a combination of PEG-IFN-α with ribavirin, does not produce SVR in all patients treated. Large-scale studies on 48-week-long PEG-IFN-α/RBV treatment in the United States and Europe showed that 42–52% of patients with HCV genotype 1 achieved SVR[2–4], and similar results were found in Japan. However, older patients (greater than 50 years of age) had a significantly lower rate of SVR due to poor adherence resulting from adverse events and laboratory-detectable abnormalities such as neutropenia and thrombocytopenia[5,6]. Specifically, various well-described side effects (such as a flu-like syndrome, hematologic abnormalities and adverse neuropsychiatric events) often necessitate dose reduction, and 10–14% of patients require premature withdrawal from interferon-based therapy[7]. To avoid these side effects in patients who will not be helped by the treatment, as well as to reduce the substantial cost of PEG-IFN-α/RBV treatment, it would be useful to be able to predict an individual's response before or early in treatment. Several viral factors, such as genotype 1, high baseline viral load, viral

[1]Department of Clinical Molecular Informative Medicine, Nagoya City University Graduate School of Medical Sciences, Nagoya, Japan. [2]Department of Human Genetics, Graduate School of Medicine, The University of Tokyo, Tokyo, Japan. [3]Division of Gastroenterology and Hepatology, Musashino Red Cross Hospital, Tokyo, Japan. [4]Department of Gastroenterology and Hepatology, Tokyo Medical and Dental University, Tokyo, Japan. [5]Division of Hepatology and Pancreatology, Kawasaki Medical College, 577 Matsushima, Kurashiki, Japan. [6]Department of Internal Medicine, Hokkaido University Graduate School of Medicine, Sapporo, Japan. [7]Molecular Gastroenterology and Hepatology, Kyoto Prefectural University of Medicine, Kyoto, Japan. [8]National Hospital Organization Osaka National Hospital, Osaka, Japan. [9]Department of Medicine, Shinshu University School of Medicine, Matsumoto, Japan. [10]Division of Gastroenterology and Hepatology, Internal Medicine, Saitama Medical University, Saitama, Japan. [11]Second department of Internal Medicine, Faculty of Medicine, Tottori University, Yonago, Japan. [12]Department of Gastroenterology, Kanazawa University Graduate School of Medicine, Kanazawa, Japan. [13]Department of Gastroenterology and Metabology, Ehime University Graduate School of Medicine, Ehime, Japan. [14]Department of Internal Medicine, Hyogo College of Medicine, Nishinomiya, Japan. [15]Central Research Laboratory, Hitachi Ltd., Kokubunji, Japan. [16]Gastroenterology and Hepatology, Yamaguchi University Graduate School of Medicine, Yamaguchi, Japan. [17]Research Center for Hepatitis and Immunology, International Medical Center of Japan Konodai Hospital, Ichikawa, Japan. [18]These authors contributed equally to this work. Correspondence should be addressed to M.M. (mmizokami@imcjk2.hosp.go.jp).

Received 29 June; accepted 21 August; published online 13 September 2009; doi:10.1038/ng.449